CHALMERS

HVDC Transmission System with Medium-Frequency Transformers

Master of Science Thesis

Adil Mohammed Elhaj

MSc in Electric Power Engineering (120 ECTS)
Department of Electric Power Engineering
Division of Energy and Environment
CHALMERS UNIVERSITY OF TECHNOLOGY
Göteborg, Sweden, 2009

HVDC Transmission System with Medium-Frequency Transformers

Adil Mohammed Elhaj

Master of Science Thesis

Supervisor:

Dr. Staffan Norrga

Examiner:

Prof. Torbjörn Thiringer

Conducted at:

ABB Corporate Research Centre, Västerås-Sweden

Department of Energy and Environment
Division of Electric Power Engineering
CHALMERS UNIVERSITY OF TECHNOLOGY
Göteborg, Sweden, 2009

Abstract

For voltage adaptation and galvanic isolation in High Voltage Direct Current (HVDC) converter stations, standard transformers operating at grid frequency are currently used. These devices tend to be very large and heavy, which is undesirable in many applications. Transformers where the magnetic parts operate at a frequency considerably higher than the grid frequency could offer many advantages. Smaller and lighter transformers and lower losses are among them.

In this thesis, a future-oriented HVDC converter station using a medium frequency MF transformer is studied with special focus on the converter circuits. The converter size used in this work is 78MW (±75kVDC/11kVAC) and the main application is power transmission to and from offshore installations. The converter consists of a snubbered Voltage-Source Converter VSC and 2-phase by 3-phase cycloconverter connected by a MF transformer. The VSC is implemented using a single phase leg and the cycloconverter is implemented using fast thyristors. It is expected that the semiconductor losses of the power conversion system will be significantly reduced by the use of the proposed converter topology which permits soft switching of all semiconductor valves in all operating points without any auxiliary valve.

The thesis evaluates the commercial potential of the proposed HVDC system. A general circuit design based on available preconditions is made first for the studied converter station, and then a comparison with an existing two-level HVDC-Light station with regard to semiconductor requirements and losses is performed for the same operating point. The total space occupied by the valve installations for both systems is also estimated. The comparison shows that the proposed system promises a considerable reduction in the number of semiconductor devices and, as a result, the total volume of the converter valves. However, the semiconductor losses increase slightly.

Key words*: Medium frequency MF transformer HVDC system, Mutually commutated converter MCC, Low frequency LF transformer HVDC system, Conventional voltage source converter VSC, Modulation ratio, Thyristor turn-off time*

I

Acknowledgement

Nomenclature

π Circular constant ($\approx$3.14159265...)   [-]

j Complex operator ($\sqrt{-1}$) [-]

t Time [s]

φ Angle of current at the grid [rad]

I_g RMS value of the current at the grid [A]

I_{cyc} RMS value of reactor current at fundamental frequency [A]

Ψ Angle of reactor current [rad]

i_i Instantaneous phase currents of cycloconverter (i=1,2,3) [A]

u_i Instantaneous voltages of cycloconverter (i=1,2,3) [V]

i_{tr} Medium frequency transformer current (VSC winding) [A]

u_{tr} Transformer voltage (VSC winding)[V]

U_d Converter DC link voltage without ripple [V]

$\boldsymbol{U_{dmaxdeblock}}$ Maximum DC link voltage when the converter is switching (including the ripple).

U_L Phase-to-phase voltage of the grid [V]

V Grid phase voltage [V]

V_{cyc} Phase voltage of cycloconverter at fundamental frequency [V]

δ Angle of cycloconverter voltage at fundamental frequency [rad]

C_s Snubber capacitance/valve [F]

k_d Coupling function for VSC[-]

$k_{ac,i}$ Coupling functions for cycloconverter phase legs[-]

L_λ Transformer leakage inductance [H]

N_{tr} Transformer turn ratio (N_2/N_1) [-]

f_{sw} Switching frequency[Hz]

f Fundamental frequency[Hz]

M Modulation index [-]

P Active power at the grid [W]

Q Reactive power at the grid [VAR]

Pf Power factor [-]

S_b Base Power [VA]

Q_{filt} AC filter reactive power [VAR]

C_f AC filter capacitor [F]

X_b Base impedance[Ω]

X_r Reactor impedance[Ω]

t_q Thyristor turn-off time[s]

di/dt Current derivative during thyristor turn-on and turn-off [A/s]

Δt_{vsc} Switching time for VSC [s]

Δt_{acci} Commutation time of a one leg of cycloconverter [s]

$N_{igbt\_w/o}$ Number of IGBTs/valve without a redundancy [IGBT]

N_{igbt} Number of IGBTs/valve with a redundancy [IGBT]

N_{diode} Number of diodes/valve [diode]

N_{valve} Number of VSC valves [valve]

N_{thy} Number of series-connected thyristors/valve [thyristor]

Contents

Chapter 1
Introduction

This chapter gives a brief introduction of the background concerning the field of the thesis. After that, the objectives and the outline of the whole work are also included in the end.

1.1 Background

A mutually commutated converter, MCC system, consisting of a voltage source converter VSC and a cycloconverter connected by a medium-frequency transformer allow bidirectional DC/AC conversion as well as voltage transformation and isolation by the transformer was proposed in [1]. Single-phase medium-frequency transformers have comparably low losses and their compact size and low weight implies an important benefit in an offshore environment. In addition, the voltage source converter is considerably simplified by the reduction to one phase leg, hence the number of IGBTs is also reduced which implies a tremendous cost saving. The cycloconverter valves do not need any turn-off capabilities and can be realized by fast thyristors connected in anti-parallel

The switching losses and stress on the semiconductor devices of power conversion systems can be considerably reduced by applying a soft-switched commutation scheme in all points of operation without any auxiliary valve. Despite the soft-switching commutation scheme, such converter systems may result in low system efficiency because they require an extra power conversion stage compared to conventional VSC converter systems.Therefore, in order to reduce the power losses in the cycloconverter, it is desirable to utilize fast thyristors instead of IGBTs since these devices have lower switching losses compared to IGBTs [7]. Nowadays thyristors are available with turn-off time (t_q) down to 5 µs which makes it feasible to use thyristor-based cycloconverters for high frequency applications. Moreover, the thyristor can handle very high current and is cheaper compared to the IGBT which implies a significant reduction in the investment cost of the cycloconverter.

However, the absence of turn-off capability of the thyristors demands for improved control strategies of the cycloconverter in order to avoid an accidental short-circuit of any phase leg of cycloconverter due to the commutation of the valves during the zero-current crossing. In [3], [4] and [12] control strategies for MCC systems equipped with thyristor-based cycloconverter were introduced. Additionally, the thyristor must be reverse biased for a certain duration t_q before a positive voltage is reapplied without unintentional self-triggering of the thyristor. This condition appears to be an even greater limitation for the operation of the cycloconverter than the absence of turn-off capability [4].

It would accordingly be of interest in this thesis to calculate the semiconductor losses for the MCC topology taking into account the turn-off time constraint of the thyristors and to compare these losses, the requirements of semiconductor devices and the size

of the valves with those of a two-level HVDC-Light system used for the same application.

1.2 Objectives

The main objective of this thesis is to estimate the semiconductor losses of an HVDC power transmission using a MF transformer or a MCC topology and to make a benchmarking with the two-level VSC technology known as HVDC-Light used for the Valhall project[1] with regard to losses, semiconductors requirements and physical volume of the equipment. The semiconductors requirements here mean the ratings, safe operating area and the number of switches.

The following steps are followed to reach the goal:
*   The theoretical concepts of both converter topologies are reviewed.
*   The preconditions for the design of the MCC topology are gathered based on data of the Valhall project[1]
*   Based on the operating conditions given in the preconditions, the design of the converter station of the MCC topology is made. The semiconductor dimensioning both for VSC part and cycloconveter part is made. The size of the AC filter reactance, MF transformer turn ratio and leakage inductor, filter capacitor and snubber capacitor of the VSC part of MCC are decided. The design values of the converter station of the HVDC-Light topology are taken from the Valhall project data
*   The semiconductor losses and the total volume of the valves are evaluated and compared for both topologies.

1.3 Outline of the thesis

Chapter 2
The preconditions for the converter station design are introduced in this chapter. Firstly, a brief description of the HVDC-light system of Valhall is made, followed by giving the requirements for the design.

Chapter 3
As the main purpose of this chapter is to describe the two compared HVDC systems, a short description of the DC/AC substations for both systems is given, the principle of operation of the studied MCC topology is explained and finally a brief explanation of the two-level conventional VSC converter is made.

Chapter 4
In this chapter, the main circuit design of the converter station for the MF transformer HVDC transmission is presented. The equations used as a basis for the design are derived first. A detailed description of different trade-offs encountered during the selection process of the semiconductors are then illustrated. The ratings of

---

1.Valhall is a power-to-shore project in the North Sea feeding oil platform which was put in operation in 2006

the proposed semiconductor devices are also given. Finally the data of the other compared HVDC topology is presented

Chapter 5

This chapter presents the simulation results of semiconductor losses for both systems. Firstly the equations used to calculate the semiconductor losses in both systems are derived. Following that, the simulation results of semiconductor losses as well as the number of valves used in both HVDC topologies are compared and different conclusions are drawn out. Finally, the total volume of the valve installations for both topologies is compared.

Chapter 6

This chapter summarizes the work in this thesis and brings forward future aims in this field

Chapter 2
Preconditions for the converter station design

This chapter gives a summary of the design requirements for the offshore converter stations of Valhall project. A short description of the transmission system which supplies the Valhall offshore installations is given, followed by the preconditions for design.

2.1 The transmission system of Valhall

The transmission system converts ac power from the Elkem's 300 kV onshore sub-station at Lista to dc power at 150 kV, transmits it through the subsea dc cable and converts it back to ac at 11 kV at the new platform to feed the entire Valhall field [8]. The HVDC is a forced-commutated Voltage-Source Converter (VSC). The HVDC transmission system between Norway and Valhall is a monopolar connection [10]. Figure 2.1 shows the transmission system designed to supply the offshore facilities at Valhall
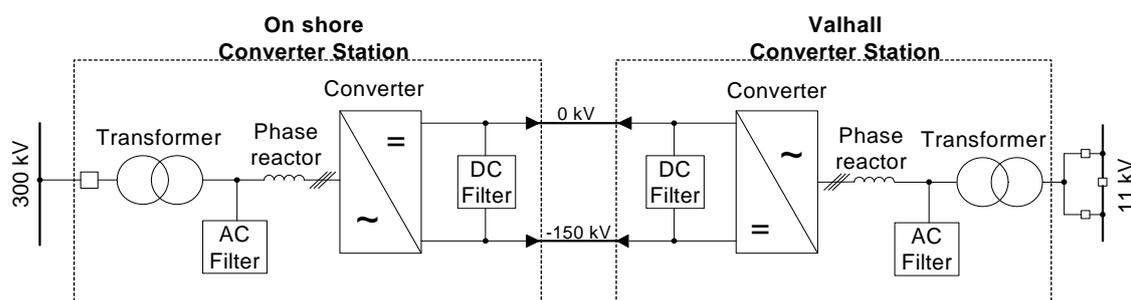
Figure 2.1. Single line diagram for the power system supplying valhall offshore platform.

2.2 Preconditions for the design

In this study the onshore station is not considered when the comparison is made between the MF transformer HVDC and LF transformer HVDC as it is independent of offshore converters. It is shown in the figure above mainly to give the reader a clear picture of the current Valhall HVDC transmission which is based on hard-switching VSC and LF transformer i.e. HVDC-Light technology.

2.2.1 Voltage, frequency and power requirements

Table 2.1 below summarizes the grid voltage, frequency and power requirements for the Valhall converter station [8]

Table 2.1. Voltage, power and frequency specifications of the Valhall offshore station

Grid voltages	DC link voltage	Power ratings	Frequency
11kVrms ±1% (steady state) 11kVrms+ 20% (fault clearance) 11kVrms-15% (starting of induction motor)	150kV	P=78MW Q=48.4MVAr (inductive) S=91.8MVA	60Hz ±0.5%(steady state) 60Hz ±10%(transient) 60Hz ±0.1Hz (with HVDC control)

The dc link voltage is 150kV as can be seen in fig 2.1. The station design for the MCC topology should be made in such a way that it meets the voltage, power and frequency requirements stated above.

2.2.2 Harmonics requirements

The maximum harmonic distortion for offshore is defined as per IEC 61000-2-4 and Class 2 is applied. The performance limits for both offshore and onshore [9] are summarized in table 2.2.

Table 2.2.Harmoics limits

Distortion factor	Harmonic number	Offshore (11kV)
D_n %	5	6
	7	5
	11	3.5
	13	3
	17	2
	17<n≤49	2.27*(17/n)-0.27
	49<n	0.2
THD %	-	8
TIF	-	-

where:

The individual harmonic voltage distortion D_n, defined as:

$$D_n = \frac{U_n}{U_1}$$

(2.1)

The total voltage harmonic distortion THD, defined as:

$$THD = \sqrt{\sum_{n=2}^{50} U_n^2} \times \frac{1}{U_1} \qquad (2.2)$$

The telephone influence factor TIF, defined as:

$$TIF = \sqrt{\sum_{n=1}^{50} \left[\frac{U_n \times TIF_n}{U_1} \right]^2} \qquad ,$$

(2.3)

where:

U_1 = nominal line to ground system voltage (rms).

U_n = n'th harmonic component of the line to ground voltage (rms).

n   = harmonic order.

TIF_n = the weighting factor of harmonic 'n' according to EEI Publication 60-68 (1960)

To meet such harmonics limits the use of filter is indispensable for both topologies (the proposed MF transformer topology and the existing HVDC-Light topology). However, since the filter design is not within the scope of this thesis it is not addressed in details when the design of MF transformer HVDC topology is made. Generally, by increasing the switching frequency it is possible to shift the dominant harmonics toward the higher frequencies and then they can be filtered out easily. Another advantage of elevating the switching frequency is the reduction of either the core area or winding area of MF transformer and hence the volume and weight of this transformer is also reduced. However, using a high switching frequency results in an increase in MF transformer winding losses due to skin effect, core losses (hysteresis and eddy current) and dielectric losses. Another drawback of increasing the switching frequency is that it results in higher semiconductors switching losses and the devices will be stressed accordingly. The application of the soft switching will result in lower switching losses in case of the MF transformer topology.

Chapter 3
Description of the two compared systems

The first part of this chapter provides a description of the two HVDC systems to be compared. A general description of the MF transformer HVDC transmission system is presented first followed by the principle of operation and modulation strategy of the MCC converter. Finally the LF transformer HVDC transmission system (HVDC-Light) together with its two-level VSC converter is explained briefly.

3.1 Description of a MF transformer HVDC transmission system

Figure 3.1 shows a block diagram of the offshore DC/AC substation for the studied MF transformer HVDC system. It consists of a VSC converter connected through a MF transformer to a thyristor-based cycloconverter. The cycloconverter terminal is connected to the grid through a phase reactor which should be large enough to smooth out the current ripples. The reactor should also give the necessary reactance to control the converter. The shunt filter is represented here by a capacitor with a main function of filtering out the harmonics of the output voltages and removing the unwanted electrical noise from the converter.
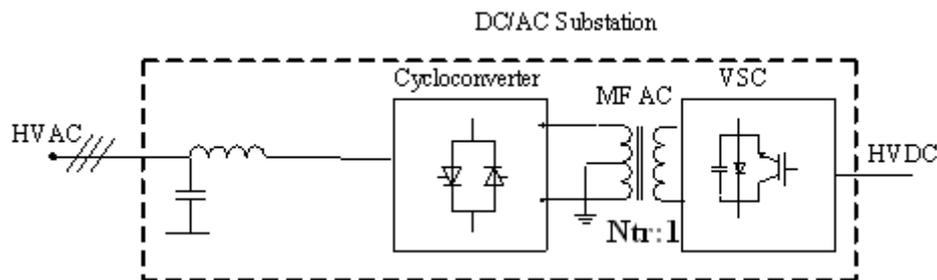
Figure 3.1. Future-oriented HVDC power transmission system including MF transformer

A zoomed picture of the VSC and cycloconverter is shown in figure 3.2. The VSC valves consist of a number of IGBT modules connected in series in order to be able to switch voltages higher than the rated voltage of a single IGBT. The series-connected IGBTs are represented in the figure by one switch. Similarly for the cycloconveter, its valves are implemented using of series-connected fast thyristors. It should be mentioned that the VSC may be realized with a single or two phase legs. In case of using a single phase leg (half bridge), the output voltage is formed between the midpoint of the phase leg and the midpoint of the two equal series-connected DC capacitors and hence it has two level: $\{U_d/2, U_d/2\}$. This option requires only two gate drive units and hence it has a big advantage compared to the two-leg option [1].

Figure 3.2. Cycloconveter and one-leg (half-bridge) VSC

On the other hand, the two-leg VSC (full bridge connection) shown in figure.3.3 has a significant advantage of establishing of three-level output voltage *{-U$_d$, 0, U$_d$}* by making the current freewheel in the converter. In addition, this type of connection provides twice the output voltage of the half-bridge. However, this difference in the output voltage can be compensated by adjusting the turn's ratio of the transformer and hence it doesn't constitute a serious limitation in a transformer coupled system [1]. Regardless of which option is used the main purpose is to convert the dc link voltage into an AC voltage with a constant frequency considerably higher than the grid frequency.
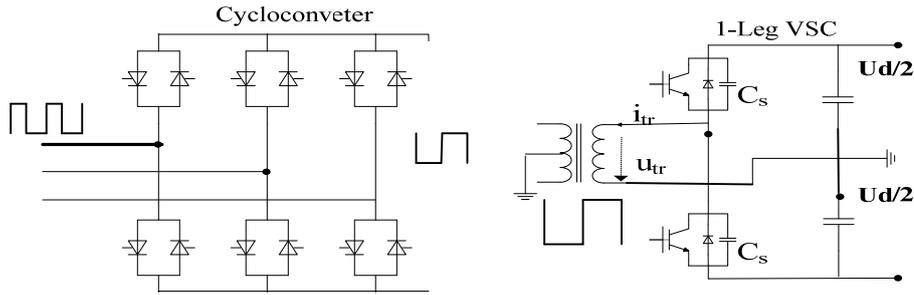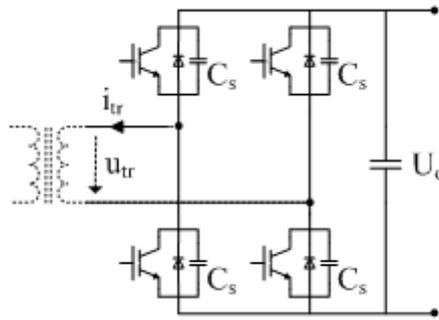

Figure 3.3. Full bridge VSC converter

3.1.1 Fast thyristors

Thyristors are inherently low switching devices due to the nature of bipolar conduction and the amount of stored charge [4]. This causes a large reverse recovery current (I_{rr}) during the turn-off which, in turn, results in a large reverse overvoltage (refer to figure 3.6). This overvoltage can be limited by connecting an RC snubber across the cycloconverter valves [4].

To shorten the turn-off time, an interdigitated gate-cathode structure is used [13]. Another way to shorten the switching times is to decrease the carrier lifetimes, with the trade-off of increasing the conduction losses. This is done by diffusing heavy metal ions or by neutron irradiation of silicon, and thereby the charge recombination ability is improved. Such fast thyristors have shorter turn-off time (t_q) which represent the minimum time before a thyristor can be exposed to a forward voltage without a risk of self-triggering by the remaining charge carriers that have not yet recombined.

Therefore, the turn-off time is usually several times longer than excess-carrier lifetimes [4].

3.1.2 Principle of MCC operation

The topology of the studied mutually commutated converter MCC system is illustrated in detail in figure 3.4. The shunt filter of the converter is ignored in this figure.
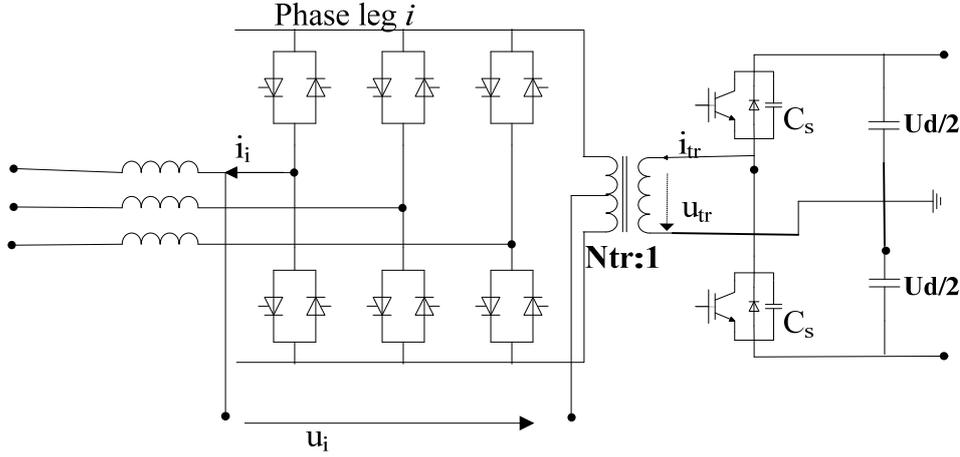
Figure 3.4 Topology of the MCC system

To simplify the analysis of the operation of the converter system different coupling factors that relate the current and voltages are introduced. Since the output voltage of the cycloconverter is referred to the midpoint of the transformer winding, a coupled factor $k_{ac,i}$ is defined. The value of the coupling factor for each phase leg is $k_{ac,i} = -1/2$, when the corresponding leg is connected to the lower transformer terminal and $k_{ac,i} = +1/2$ when is connected to the upper transformer terminal [1].

Thus follows:

$$u_i = k_{ac,i} \, u_{tr} \, N_{tr} \tag{3.1}$$

and

$$i_{tr} = N_{tr} \Sigma k_{ac,i} \, i_i \tag{3.2}$$

Similarly a coupling factor k_d can be defined to relate the dc link voltage with the output voltage of the VSC. It has two values: $+1/2$ when the upper valve conducts and $-1/2$ when the lower valve conducts. Thus

$$u_{tr} = k_d \, U_d \tag{3.3}$$

Several important assumptions are made during each commutation cycle for the following analysis. Firstly, the AC side inductive filter is assumed to be large enough to be able to maintain the current constant in each modulation interval and hence it can be represented by a current source. Secondly, the voltage on the VSC side is

assumed to be essentially constant, which is supplied by the DC link capacitors. Finally, the transformer is modeled by its turns ratio N_{tr} and leakage inductance L_λ i.e. the small magnetizing current is neglected in order to simplify the circuit [1].

As mentioned before the name of the MCC converters comes form the fact that the VSC and cycloconverter always alternately commutate, thereby both snubbered /zero-voltage commutation and natural commutation are enabled for the first and the latter respectively [12].

Cycloconverter commutation

The only way to turn off a conducting thyristor is to let the anode current fall below the holding current. Therefore, to initialize the natural commutation of each leg of the cycloconveter equation (3.4) has to be fulfilled.

$$u_{tr} k_{ac,i} \, i_i < 0 \tag{3.4}$$

Condition (3.4) is fulfilled when the voltage applied to a thyristor in any leg becomes opposite to the direction of the anode current. This makes it possible to turn-off that thyristor. Figure 3.5 schematically shows an example of such a commutation.
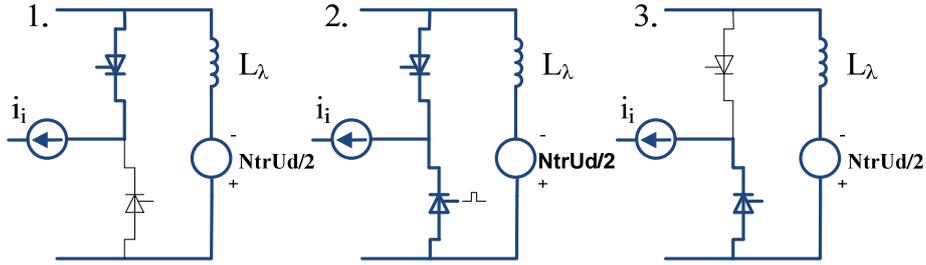
Fig. 3.5 Cycloconverter phase leg natural commutation [1]

As can be seen in figure 3.5, the current of the corresponding phase leg of the cycloconverter and the voltage across the leakage inductance are opposite to each other in direction. The process is started by turning on the non-conducting thyristor valve in the direction of the current through the phase terminal. The incoming valve gradually takes over the current. Finally the initially conducted valve turns off as the current through it drops to zero [1]. At the end of the commutation the sign of the product in (3.4) changes and a new condition for the next commutation is established.

$$u_{tr} k_{ac,i} i_i > 0 \tag{3.5}$$

When all of the cycloconverter phase legs have been commutated it follows from (3.3) and (3.5) that

$$u_{tr} i_{tr} = \text{Ntr} \sum_i u_{tr} k_{ac,i} i_i = \text{Ntr} \sum_i \frac{1}{2} |u_{tr}| |i_i| \tag{3.6}$$

10

The sign of this expression is positive which means that u_{tr} and i_{tr} are of the same sign, i.e. the instantaneous power flow is directed form the DC side to the AC side [1].

The ideal duration of cycloconverter commutation depends on the leakage inductance of the transformer (L_λ) and the output voltage of the VSC and can be found using (3.7) [5].

$$\Delta t_{acci} = L_\lambda i_i / (N_{tr} U_d / 2)$$ (3.7)

It is important to ensure that the thyristor has completely turned off before the forward voltage is applied again across it. This can be done by two measures. Firstly, the turn-off time (*tq*) specified by manufactures should be respected (refer to figure 3.6).This can be ensured by not allowing any phase leg commutation during the time period *tq* prior to VSC commutation. Secondly, the voltage derivative *dv/dt* of reapplied forward voltage across must be limited to a certain limit by snubber capacitors. Otherwise the device may retrigger into conduction-state by induced displacement current [4], and this results in commutation failure.
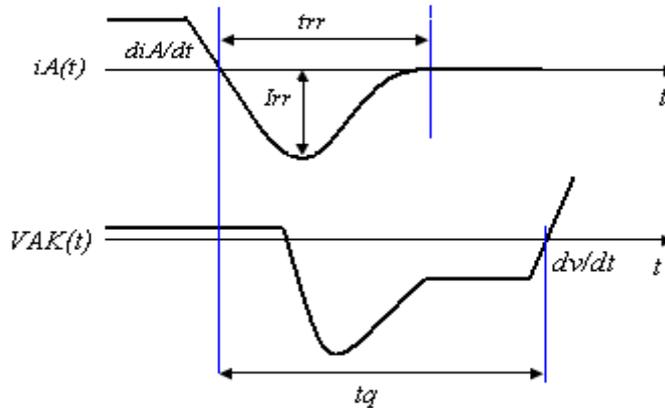
Figure 3.6. Thyristor current and voltage waveforms during turn-off [13]

It will be seen in following chapters that the increase in the turn-off time of the thyristors causes a reduction in the maximum possible modulation ratio of the converter.

VSC commutation

The commutation stages of the snubbered VSC are shown in Figure 3.7 is initiated after the cycloconverter commutation. Equation (3.6) implies that u_{tr} and i_{tr} are of the same sign which indicates that the current flows through the switches instead of diodes at this stage (refer to figure 3.7).
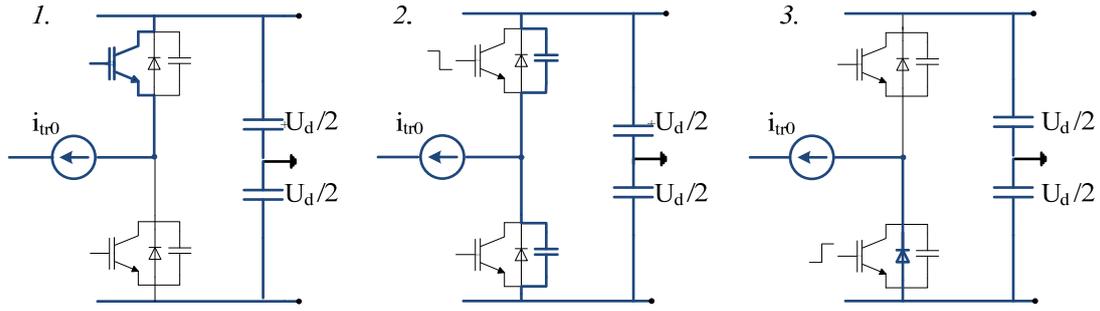
Fig. 3.7 Snubbered VSC commutation [1]

The commutation process is started by turning off the conducting switch at zero-voltage condition; the current is diverted to the snubber capacitors (second diagram in Fig.3.7). The snubber capacitors are getting recharged until the potential of the phase terminal has fully moved to the opposite DC rail. At this moment, the snubber capacitors in the incoming valve are completely discharged and the current follows through the diode in the opposite valve. Finally, the switch connected in anti-parallel to this diode is turned on at zero-voltage and zero-current conditions. The next current direction reversal is established by turning on this switch. At the same time, the reversal of the transformer voltage u_{tr} during the VSC commutation establishes a condition for natural commutations of the cycloconverter phase legs. Therefore, the commutation cycle can be repeated [1].

The VSC commutation time Δt_{vsc} is governed by the snubber capacitor per valve and the transformer current thus

$$\Delta t_{vsc} = 2C_s U_d / i_{tr} \qquad (3.8)$$

Fig 3.8 shows the current and voltage waveforms during a couple of commutation cycles. The duration of commutation process has been exaggerated in the figure just for clarity. In reality the commutation time is only a very small fraction of the commutation cycle [1]. The time period t_q corresponds to manufacture-specified turn-off time of thyristor as discussed in the last part of the previous paragraph.
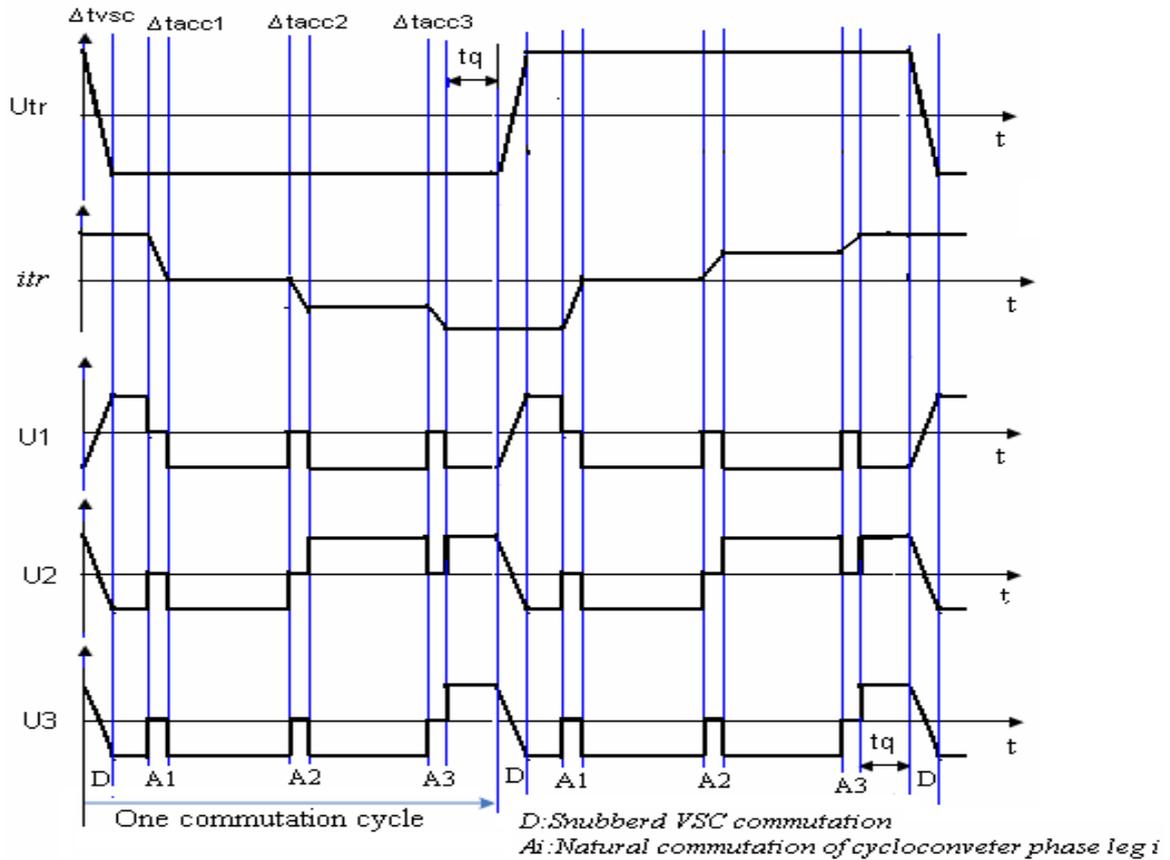
Fig.3.8. Current and voltage waveforms during commutation sequence as given in [1]

Modulation

In addition to maintaining soft switching, the control of the MCC system should fulfill two main requirements. Firstly, a proper operation of the transformers should be ensured by avoiding low frequency or DC components in the transformer voltage. This can be achieved by fixed VSC commutation intervals, thus generating a trapezoidal voltage. Secondly, the control system should produce the desired PWM patterns for the cycloconverter. By making the commutations of the cycloconverter phase legs at appropriate instants in the interval between two VSC commutations, the width of the PWM pulses can be chosen freely [1]. This may be achieved in several ways. In this thesis a carrier-based modulation method is used. This modulation scheme is called a constrained sinusoidal pulse width modulation (SPWM) and is treated extensively in [1]. Figure 3.9 shows how this modulation scheme works for a couple of cycles. Two sawtooth carriers are used one for the positive phase current and the other for the negative current. The waveforms below are shown for a case where the current of the first phase is positive while the currents of the other two phases are negative.

13
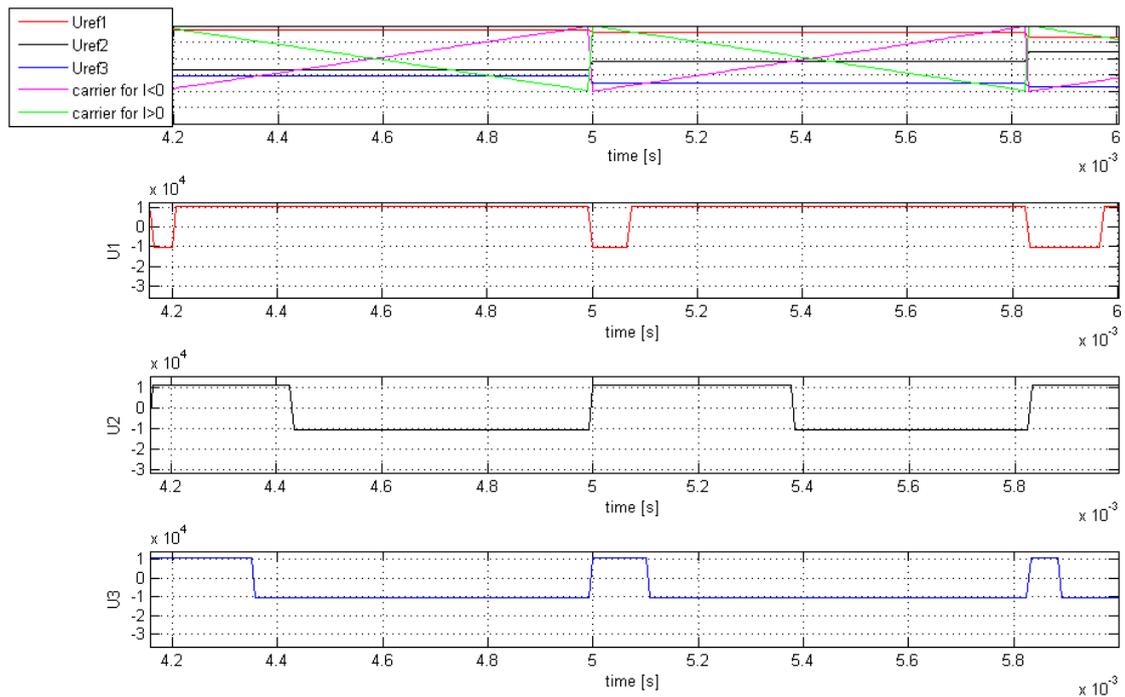
Figure 3.9 References, sawtooth carriers and output AC voltages of cycloconverter

3.2 Description of a state-of-the-art LF transformer HVDC transmission system (HVDC-Light)

A block diagram of the DC/AC substation of the LF transformer HVDC system is shown in figure 3.10. It consists of a two-level VSC converter connected through a reactor to a LF transformer. The shunt filter consists of an inductor, a capacitor and a resistance. The main function of the filter and the reactor is the same like the one described in section 3.1. Besides adjusting the voltage between the grid and the converter, the secondary-grounded star-star transformer blocks the zero-sequence harmonics from being injected into the grid. This system resembles the current offshore substation which supplies Valhall installation.
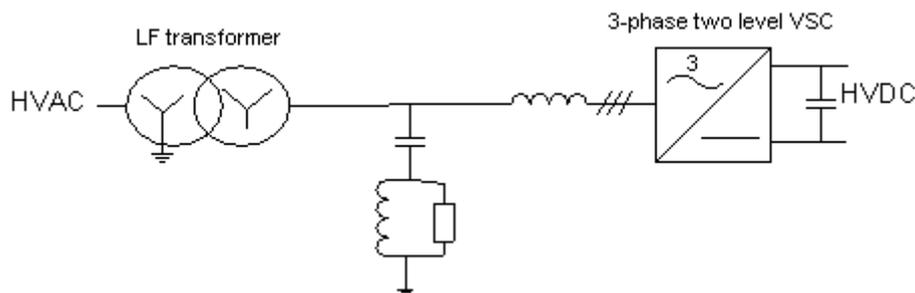
Fig.3.10. Conventional VSC-based HVDC system with a LF Transformer

14

3.2.1 The two-level conventional VSC

A detailed diagram of the 3-phase two levels VSC of figure 3.10 is shown in figure 3.11. Each valve consists of large number of series-connected IGBT modules since it is required to block a voltage as high as the dc link voltage. The most important thing is that all IGBTs must turn on and off at exactly the same moment. The commutation takes place alternately between the IGBTs in the upper legs and the diodes in the lower legs and vice versa. The positive current is conducted by the IGBTs in the upper legs together with the diodes in the lower legs and vice versa for the negative current. The output voltage is switched between two voltage levels and is generated by a PWM control.
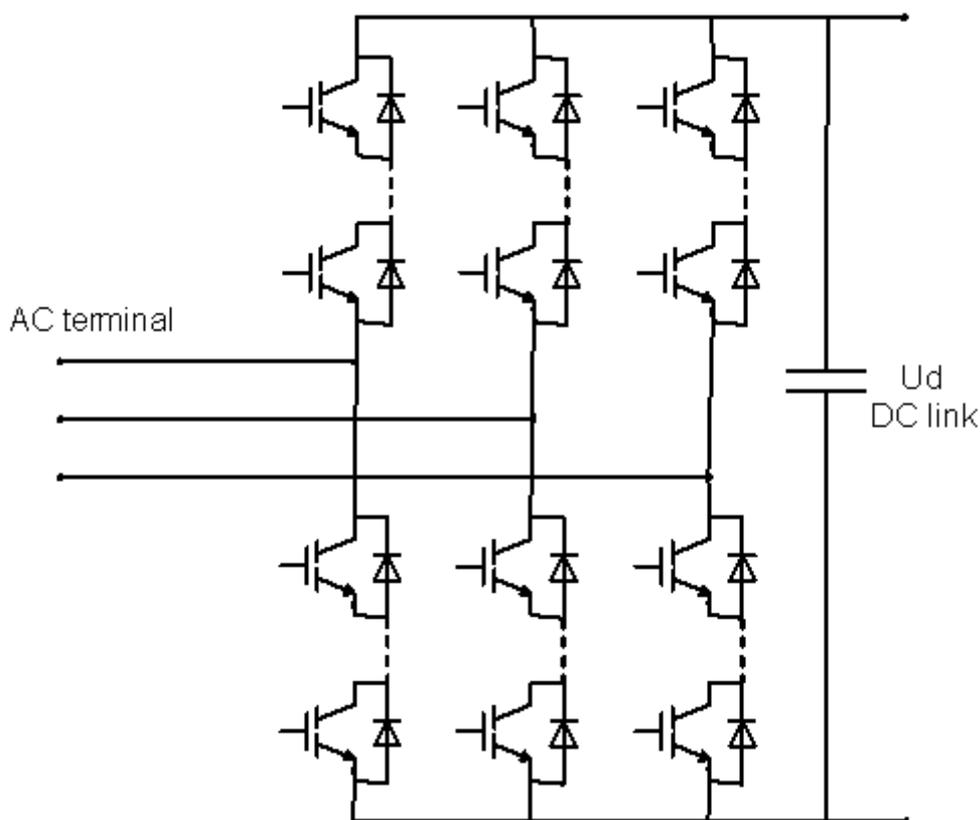
Figure 3.11. Three-phase two-levels VSC

This type is converter is called hard-switching since the semiconductor devices are subjected to a high current and high voltage simultaneously during a substantial part of the switching process. Therefore, the converter has higher switching losses compared with its MCC counterpart as will be shown later.

Chapter 4
Converter station design

This chapter presents a rough design of the DC/AC converter station for the studied MF transformer HVDC system with special focus on the semiconductor ratings. The derivation of the equations used as a basis for the design is made first. Following that, different compromises have to be considered during the selection process of semiconductor devices are discussed. Finally, the main circuit data and semiconductor characteristics of the other compared topology are presented.

4.1 Converter station design for the MF transformer topology

4.1 .1 Main important assumptions

- The magnetizing current and the winding resistance of the transformer windings are neglected and hence the transformer is represented by solely its turn ratio and leakage inductance.
- The resistive together with the inductive reactance of the AC side shunt filter is small compared to its capacitive reactance at the fundamental frequency. Therefore the shunt filter can be represented by a pure capacitor at that frequency.
- The internal resistance of the AC side reactor is negligibly small value and hence the reactor can be modeled by a pure inductor.

4.1.2 Basic equations for the design

Figure 4.1 shows a one-phase equivalent circuit of the AC side of the converter station (figure 3.1) of the MCC at the fundamental frequency based on the second and third assumption. The load connected to the grid is represented by the resistance R and the inductance L.
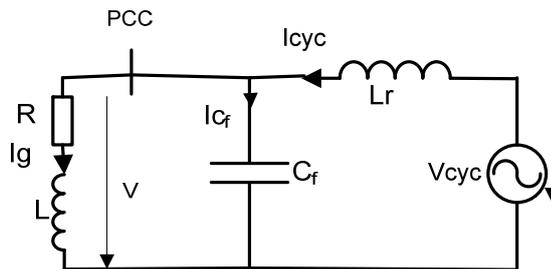

Fig.4.1 Single phase equivalent of the AC side

The cycloconverter output voltage at the fundamental frequency V_{cyc} can be calculated by

$$V_{cyc} = V + jX_r I_{cyc} \tag{4.1}$$

where

$$I_{cyc} = I_{Cf} + I_g \tag{4.2}$$

$$I_{cyc} = jY_c V + (P - jQ)/(3V) \tag{4.3}$$

The impedance of the reactor is taken as 15% of the base impedance X_b since it should be big enough to smooth out the inductor current and to limit the high transient current derived by the energy stored in the big rotating machines connected to the AC grid in case of a short-circuit in the dc-link.

$$X_r = 2\pi f L_r = 0.15 X_b \tag{4.4}$$

The admittance of the shunt filter can be calculated from the reactive power supplied by the filter (Q_{filt}) and the grid voltage. In general the filter size should be as small as possible. The experience has shown that a value of 15% of the base power S_b could be satisfactory for Q_{filt} .

$$Y_c = 2\pi f C_f = Q_{filt}/(3V^2) = 0.15 S_b/(3V^2) \tag{4.5}$$

The modulation ratio (M) is defined as a ratio of the peak value of the cycloconverter phase voltage to half of the transformer secondary voltage during one commutation cycle.

$$M = \sqrt{2}\left|V_{cyc}\right|/(N_{tr}U_d/4) \tag{4.6}$$

The maximum modulation ratio can be calculated from figure 3.8 for any leg using

$$M_{max} = 1 - 2f_{sw}(\Delta t_{vsc} + \Delta t_{acc1} + \Delta t_{acc2} + \Delta t_{acc3} + 2t_q) \tag{4.7}$$

If the commutation of the first leg takes place at the peak value of the phase current, then the commutation time for that leg can be calculated as

$$\Delta t_{acc1} \approx \sqrt{2}\left|I_{rms\_cyc}\right|/(di/dt) \tag{4.8}$$

And the commutation time for the other two phase legs can also be approximated by

$$\Delta t_{acc2} \approx \Delta t_{acc3} \approx 0.5\Delta t_{acc1} \tag{4.9}$$

The switching of the VSC occurs near the peak value of the phase current (at fundamental frequency) of a cycloconverter leg while the currents of the other two legs have different signs compared to this leg's current .Thus using (3.2) and (3.8), the switching time of VSC can be roughly estimated by

$$\Delta t_{vsc} \approx 2C_s U_d /(N_{tr}\sqrt{2}\left|I_{cyc}\right|) \tag{4.10}$$

From (4.6), (4.7) and (4.10), and by assuming that the converter is operating at the maximum modulation ratio, the minimum required transformer turns ratio N_{tr} can be calculated as

$$N_{tr} = (2k_1 f_{sw} + k_2)/(1 - 2f_{sw}(\Delta t_{acc1} + \Delta t_{acc2} + \Delta t_{acc3} + 2t_q)) \tag{4.11}$$

where

$$k_1 = 2C_s U_d /(\sqrt{2}|I_{cyc}|) \tag{4.12}$$

$$k_2 = 4\sqrt{2}|V_{cyc}|/(U_d) \tag{4.13}$$

Finally leakage inductance of the transformer can be estimated from

$$L_\lambda = (N_{tr} U_d /2)/(di/dt) \tag{4.14}$$

The maximum allowed commutation rate di/dt is found in the thyristor data sheet. Throughout the analysis it is assumed that the max possible modulation ratio is constant, but in reality it varies slightly between different commutations intervals as a result of the variation of the cycloconverter as well as the VSC commutation times.

The total number of the series-connected IGBTs per VSC valve can be calculated by [11]

$$N_{igbt\_w/o} = U_{d\max deblock}/(V_{CE,SSOA,\max} - \Delta U) \tag{4.15}$$

The maximum dc link voltage when the converter is switching including the ripple ($U_{dmaxdeblock}$) is taken as 116% of the nominal dc link voltage (U_d) for a voltage source converter [11]. The maximum switching safe operating area voltage ($V_{CE,SSOA,max}$) is usually taken as 60% of the maximum collector-emitter voltage (V_{CEmax}). The reason for this will be explained later. The factor ΔU is mainly to account for a possible uneven distribution of the voltage among the IGBTs at a certain valve and it varies linearly with V_{CEmax}. For a 2.5kV IGBT it has a value of 275V [11]

A redundancy of 6% is then added to the number of devices [11] which gives

$$N_{igbt} = 1.06 N_{igbt\_w/o} \tag{4.16}$$

Having (4.16), it is possible to calculate the rated switching safe operating area voltage of a single IGBT in the VSC valve as

$$V_{CE0,ssoa} = U_d / N_{igbt} \tag{4.17}$$

The number of series-connected thyristors per one valve of the cycloconverter can then be calculated using:

$$N_{thy} = 2.5 U_{ov\_pk} / V_{RRM} \tag{4.18}$$

U_{ov_pk} is the maximum peak operating voltage across the valve and V_{RRM} is the maximum voltage that the thyristor can block during the switching. The experience has shown that the number of thyristors calculated in (4.18) is an acceptable level for the thyristor control reactor (TCR) valves within ABB.

The voltage U_{ov_pk} can be calculated from the transformer turn ratio and the maximum dc link voltage $U_{dmaxdeblock}$

$$U_{ov\_pk} = N_{tr} U_{d\,max\,debloc} / 2 \tag{4.19}$$

Using the number of thyristors in (4.18), it is possible to calculate the rated safe operating area voltage of the thyristor

$$V_{thy,ssoa} = N_{tr} U d / (2 N_{thy}) \tag{4.20}$$

4.1.3 Realization of the design

It is worth mentioning that the value of P and Q in (4.3) has been taken as the rated power of the Valhall offshore station (refer to table 2.1), the base power has been taken similar to the magnitude of apparent power injected into the grid and hence it can be calculated from P and Q value. The grid phase voltage (V) has been taken as $11/\sqrt{3}$ kV. The VSC of the MCC has two voltage levels either +75kV or -75kV. Table 4.1 summarizes the operating point data that can be used together with the above equations to make the converter design

Table 4.1.The rated operating point for the converter station

P[MW]	Q[MVAR]	S_b[MVA]	V[kV]	f[Hz]	HVDC voltage level
78	48.4	91.8	$11/\sqrt{3}$	60	$\pm 75kV$

The peak value of the reactor current at rated operation (Table 4.1) is 6335A.

Dimensioning of the cycloconverter semiconductors

Different thyristors with different turn-off times have been proposed. The thyristors must be selected in such a way that their current ratings are well above the rating of the reactor current by a sufficient margin. This margin is necessary in order to protect the valves against the ripple in the current (esp. at low switching frequency) or any accidental transient current. In additions to the ratings requirements, the thyristors should also be fast enough to have a high modulation index (see (4.7)) and hence a lower transformer turn-off ratio N_{tr} (refer to (4.6)) since the latter is an important factor for the dimensioning of the VSC part of the converter as will be seen later. Another important criterion for thyristors is that they should also possess high voltage blocking capability so as to reduce the number of required devices and thereby the

size of the station as will be seen in the next chapter. Nevertheless, the very fast thyristors mostly have low blocking voltage and vise versa for the slow thyristors. Therefore, a trade-off should be made between the blocking voltage and turn-off time when a thyristor is chosen.

The graph in figure 4.2 shows a plot of the maximum modulation index and transformer ratio respectively as a function of switching frequency for three thyristors with different turn-off times and the same commutation rate (di/dt). The data for the thyristors can be found in table 4.2
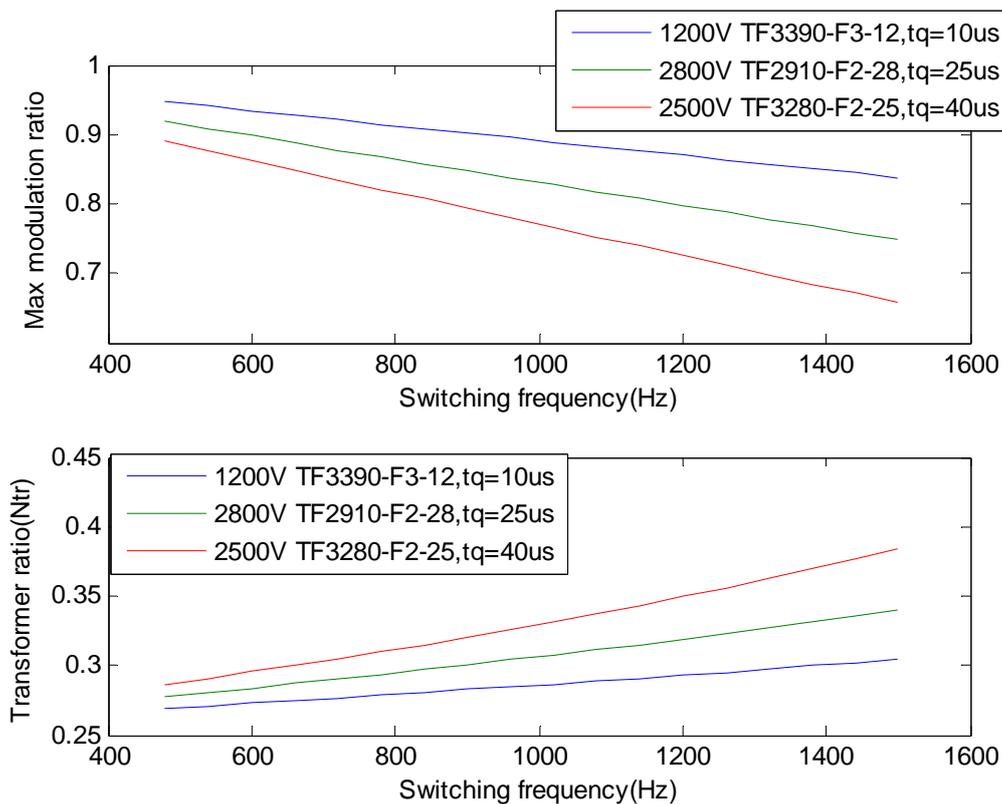

Figure 4.2. The maximum modulation index and transformer ratio at different thyristor turn-off times

It is quite obvious from the upper diagram that using slow thyristors results in large area losses in the modulated voltage (the maximum modulation index decreases) during commutation, see figure 3.8.The situation becomes even worse when the switching frequency is getting higher. The consequence of the reduction of the maximum modulation is that a higher turns-ratio of the transformer (N_{tr}) is needed to get the required AC side voltage if the slow thyristors are to be used (refer to the lower part of figure 4.2). It is clear from (3.2) that a high turn ratio results in a high peak transformer current which implies that semiconductors with high current ratings must be used to design the VSC. Increasing the switching frequency also worsens the situation and may boost the semiconductor losses.

Another compromise has to be considered when a thyristor is selected from a family of thyristors with the same blocking voltage is that the devices with a shorter turn-off time have a higher on-state voltage drop (and thereby larger conduction losses) than the ones with a longer turn-off time (see figure 4.3).
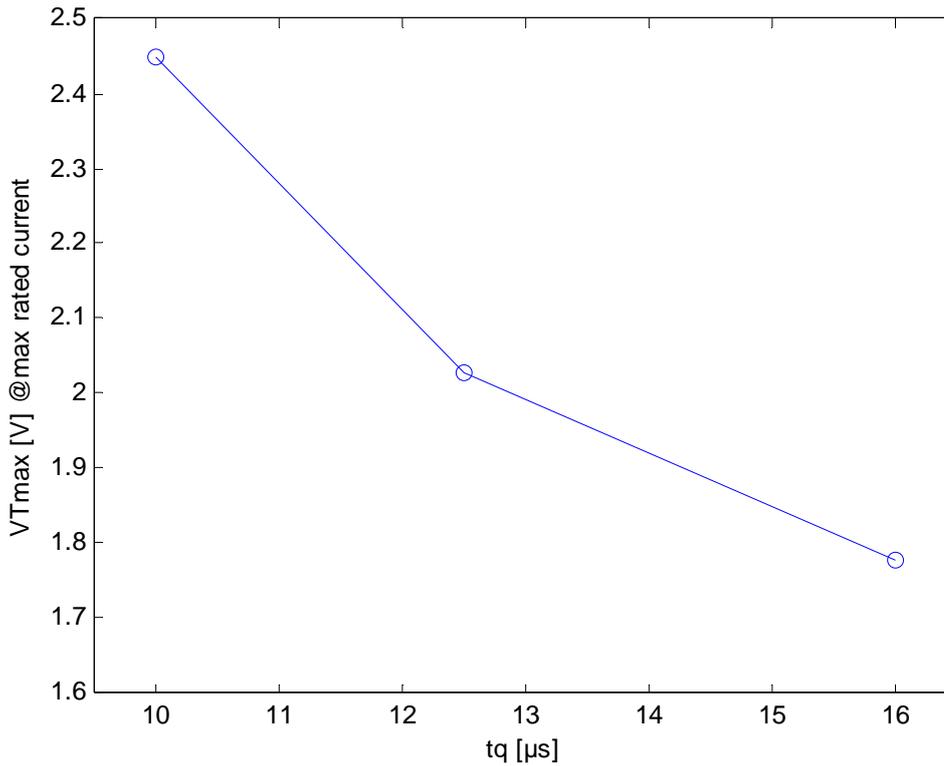
Figure 4.3. The maximum voltage drop as a function of turn-off time for thyristors with a same blocking voltage and different turn-off times

Characteristics of the proposed thyristors

Table 4.2 presents the characteristics of the thyristors proposed to be applied in cycloconverter. The thyristors are from Proton-Electrotex [14]

Table 4.2 Characteristics of the proposed thyristors

Thyristor module	TF3390-F3-12	TF2910-F2-28	TF 3280-F2-25
Peak on-state current	10.65kA	9.14kA	10.30kA
Repetitive peak off-state voltage V_{DRM}	1200V	2800V	2500V
Repetitive peak reverse voltage V_{RRM}	1200V	2800V	2500V
Rated SSOA voltage $V_{thy,ssoa}$	407 V	936 V	856V
Turn-off time t_q	10μs	25μs	40μs
On-state threshold voltage V_T	1.4V	1.4V	1.3V
On-state slop resistance r_T	0.08 mΩ	0.2mΩ	0.15mΩ

Looking at the current rating of the proposed thyristors given in the table above, it is clear that they have current ratings with a margin of more than 50% above the peak reactor current i.e. 6335A. The value of the peak reactor current is calculated using (4.3) and the converter rated operating point presented in table 4.1. The thyristor rated SSOA voltage can be calculated by using (4.20). From the values in the table, it can be noticed that a large margin between the maximum blocking voltage (V_{RRM}) and the rated SSOA voltage is taken in order to ensure that the system will remain functional

even if some thyristors at a certain valve fail to trigger and to ensure that the devices are well protected against the possible switching and lightning overvoltages or the overvoltages caused by the ripple of the dc link voltage.

Transformer ratio, leakage inductance

The value of the transformer turn ratio and leakage inductance can be evaluated using (4.11) and (4.14) respectively. The maximum current derivative during the turn-on and turn-off (di/dt) is taken from the thyristor data sheet and it has a value of 500A/μs (see appendix A).

Table 4.3 shows some values at operating switching frequency f_{sw}=900Hz for different thyristor options. The switching frequency is chosen to be 900Hz since the converter is expected to have a good harmonics performance at this frequency if it is modulated by a constrained SPWM.

Table 4.3 Transformer leakage inductance and turn-ratio at f_{sw}=900Hz

Thyristor module	f_{sw}	di/dt	L_λ	N_{tr}
TF3390-F3-12	900Hz	500A/ μs	42.4μH	0.283
TF2910-F2-28	900Hz	500A/ μs	45.0 μH	0.300
TF 3280-F2-25	900Hz	500A/ μs	48.0 μH	0.320

Obviously the above values, as can be seen from equation (4.14) and figure 4.2, vary with the switching frequency at which the converter is designed to operate and the turn-off time of the thyristor.

It is worth mentioning that the exact physical value of the leakage inductance depends on the winding geometry.

Dimensioning of the VSC semiconductors

The IGBT module is selected based on the transformer current and the dc link voltage. The transformer current determines the current ratings of the devices while the voltage ratings as well as the number of series-connected IGBT modules are decided based on the maximum value of the dc link voltage. The selected IGBT module should be able to handle a current which is higher than the rated transformer current with a sufficient margin to account for the current ripple and current increase due to transients. Up to a switching frequency of 1.2 kHz it was found that the peak of the transformer current (without ripple) doesn't exceed 2.3kA if a thyristor with tq=40μs is used.

The rated switching safe operating area SSOA voltage combined with the long term stability defines the IGBT module rating. In order to improve reliability and to avoid the device failure due to cosmic radiation the maximum allowed SSOA voltage is derated by 40% from the maximum collector-emitter voltage of the device V_{CEmax} (this de-rating margin is an acceptable figure for a 2.5kV IGBT within ABB). Again there is a margin between the maximum and rated SSOA to account for the voltage spike caused by diode reverse recovery [6]. Based on the previous discussion, the number of series-connected IGBTs per valve and thereby the rated SSOA voltage ($V_{CE,SSOA}$) can

be calculated using (4.15), (4.16) and (4.17). The ripple in the dc link voltage has also been accounted for in this calculation (refer to equation (4.15)).

To meet the discussed rating requirements, an IGBT module with the characteristics given in table 4.4 has been proposed for the VSC design. It is the 5.2kV 2000A Soft-switching IGBT module used in ABB Project Light C [15]. The device can handle a current up to 4000A (peak value).The current rating is the same for the IGBT and the diode in the same module. The value of the snubber capacitor is chosen to be 3μF/IGBT module as in Project Light C [15].

Table 4.4. Main characteristics of a 5.2kV 2000A Soft-switching IGBT module

Max. collector-emitter voltage V_{CEmax}	5.2kV
Max SSOA voltage $V_{CE,SSOA,max}$	3.12kV
Rated SSOA voltage $V_{CE,SSOA}$	2.42kV
Nominal collector current I_C	2000A
Maximum collector current I_{CM}	4000A
Diode forward current I_F	2000A
Maximum pulsed forward current I_{FM}	4000A
IGBT threshold voltage V_{CE0}	1.7V
IGBT slope resistance r_{CE}	1.15mΩ
Diode threshold voltage V_F	1.1V
Diode slope resistance r_F	0.65mΩ

4.2 Converter station design for the HVDC-Light topology

4.2.1 Design data of the converter station

Main circuit parameters

Table 4.5 gives the main circuit data of the compared HVDC-Light topology used in this study. These data can be found in [8]

Table 4.5 Main circuit data of Valhall offshore station

Base power defined at max reactor current and nominal filter voltage	94.8MVA
DC link voltage	150kV
Converter reactor size	24mH
AC filter size	8.8MVAR/4.41μF
Modulation ratio range	0.56-0.76
Max reactor current at steady state (rms)	760A
Nominal filter voltage	72kV
Transformer rated power	91MVA
Transformer turn-ratio (valve/line side)	68/11
Nominal frequency	60Hz

Semiconductors dimensioning for the conventional VSC

A two-level VSC converter similar to the one in figure 3.11 is used. A 2.5kV Press-pack IGBT, PG4 module has been used in this study to design the conventional VSC. Table 4.6 gives an overview of the device characteristics [16]. It can be noticed that this IGBT is able to handle a current (2600A) which is about twice the maximum peak reactor current (1075A). The calculation of the maximum reactor current was made in [8] and is shown as an rms value in table 4.5. The large margin between the maximum reactor current and the maximum current the IGBT can handle is needed to protect the device against any possible overcurrent caused by the starting of large induction machines, ripples or other possible transients. A similar margin is used for the 2.5kV devices used in the current Valhall offshore converter [11]. The current rating is the same for the IGBT and the diode in the same module. Similar as before, the rated switching safe operating area (SSOA) voltage can be estimated using (4.15), (4.16) and (4.17).

Table 4.6. Main characteristics of a 2.5kV Press-pack IGBT module
5SNA 130025H0003 (PG4 Light B) [14]

Max. collector-emitter voltage V_{CEmax}	2.5kV
Max SSOA voltage $V_{CE,SSOA,max}$	1.5kV
Rated SSOA voltage $V_{CE,SSOA,}$	0.99kV
Nominal collector current I_C	1300A
Maximum collector current I_{CM}	2600A
Diode forward current I_F	1300A
Maximum pulsed forward current I_{FM}	2600A
IGBT threshold voltage V_{CE0}	1.14V
IGBT slope resistance r_{CE}	1.2mΩ
Diode threshold voltage V_F	1.05V
Diode slope resistance r_F	0.57mΩ

Chapter 5
Semiconductor losses formulation, simulation results and analysis

5.1 Formulation of semiconductor losses for the Mutually Commutated Converter (MCC)

5.1.1 VSC losses

The on-state losses depend on the current through the device (I_{CE}) as well as the on-state voltage drop. They can be calculated from the threshold voltage, the on-state slope resistance and the current through the IGBT or diode. The values of the device threshold voltage and slope resistance are taken from data sheet at temperature of 125 C, and hence no temperature dependence is considered. The IGBT on-state losses can be calculated by

$$P_{cond\_igbt} = f \int_{t=0}^{1/f} I_{CE}(V_{CE0} + r_{CE}I_{CE})dt \tag{5.1}$$

Similarly, the diode on-state losses can be calculated by

$$P_{cond\_diode} = f \int_{t=0}^{1/f} I_F(V_F + r_F I_F)dt \tag{5.2}$$

The switching losses consist of turn-on and turn-off losses. The turn-on losses of the IGBTs are neglected since the turn-on takes place at zero current and zero voltage conditions. Thus the turn-off losses are assumed to be the only component of the IGBTs switching losses and can be calculated (by interpolation) from the turn-off energy curves at the corresponding turn-off current. The turn-off energy curves can be found in the device data sheet [15]. In this calculation the turn-off energy data is taken at a temperature of 125C. Having these curves, it is possible to extract the instantaneous turn-off energies by interpolation. The current through the upper valve of the VSC (I_{s1}) is shown in figure 5.1. The switching losses are the average of the instantaneous turn-off energies over one cycle of the fundamental frequency.

$$P_{sw\_igbt} = f \sum_{x=1}^{f_{sw}/f} E_{off}(I_{off}) \tag{5.3}$$

The diode turn-on takes place every cycle right after the reversal of the VSC transformer voltage (see the diode current I_{D2} in fig 5.1). The diode turn-on losses can be calculated in a similar way as the IGBT turn-off losses using the turn-on energy diagrams in the data sheet

$$P_{di\_on} = f \sum_{x=1}^{f_{sw}/f} E_{on}(I_{on}) \tag{5.3}$$

Similarly, the diode turn-off losses can be calculated using the reverse recovery energy data

$$P_{di\_off} = f \sum_{x=1}^{f_{sw}/f} E_{rec}(I_{offd}) \qquad (5.4)$$

From (5.3) and (5.4) the switching losses per a single diode can be evaluated

$$P_{sw\_di} = P_{di\_off} + P_{di\_on} \qquad (5.5)$$

Using the above equations together with the number of IGBTs per valve and number of VSC valves, the total VSC conduction losses can be calculated as

$$P_{cond\_vsc} = 2N_{igbt}P_{cond\_igbt} + 2N_{diode}P_{cond\_di} \qquad (5.6)$$

And similarly the total VSC switching losses are

$$P_{sw\_vsc\_soft} = 2N_{igbt}P_{sw\_igbt} + 2N_{diode}P_{sw\_di} \qquad (5.7)$$

The number of IGBTs or diodes per valve can be calculated using (4.16). The number of diodes per valve N_{diode} is taken the same as the number of IGBTs for the selected IGBT module. The subscript ''soft ''in (5.7) stands for soft switching.
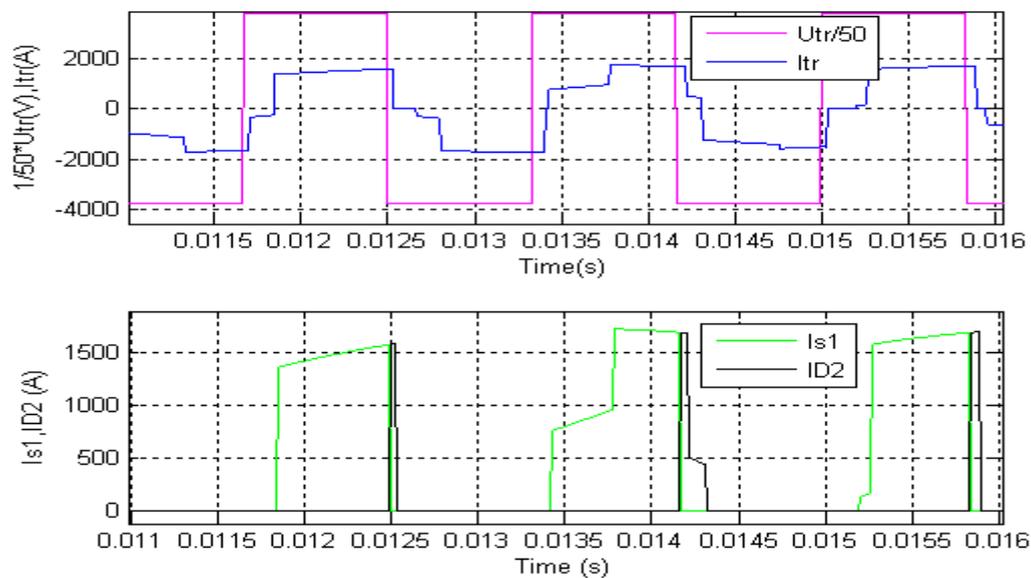

Figure 5.1 Simulated transformer voltages (magenta), transformer current (blue) upper IGBT current (green), lower diode current (black) during a few number of cycles

5.1.2 Cycloconverter losses

The conduction losses of the thyristor can be calculated by

$$P_{cond\_thy} = f \int\limits_{t=0}^{1/f} I_{thy}(V_T + r_T I_{thy})dt \qquad (5.8)$$

I_{thy} is the current through one thyristor at the upper or lower valves of one cycloconverter leg. Figure 5.2 shows a plot of this current together with the cycloconverter phase voltage and current. It should be mentioned that the current ripple is ignored when the loss calculation is made in this study.

The thyristor manufactures usually provide the thyristor losses (including conduction and switching) as a total energy losses at a given conduction time, commutation rate, voltage and at different values of the device current as can be seen from figure 5.3.
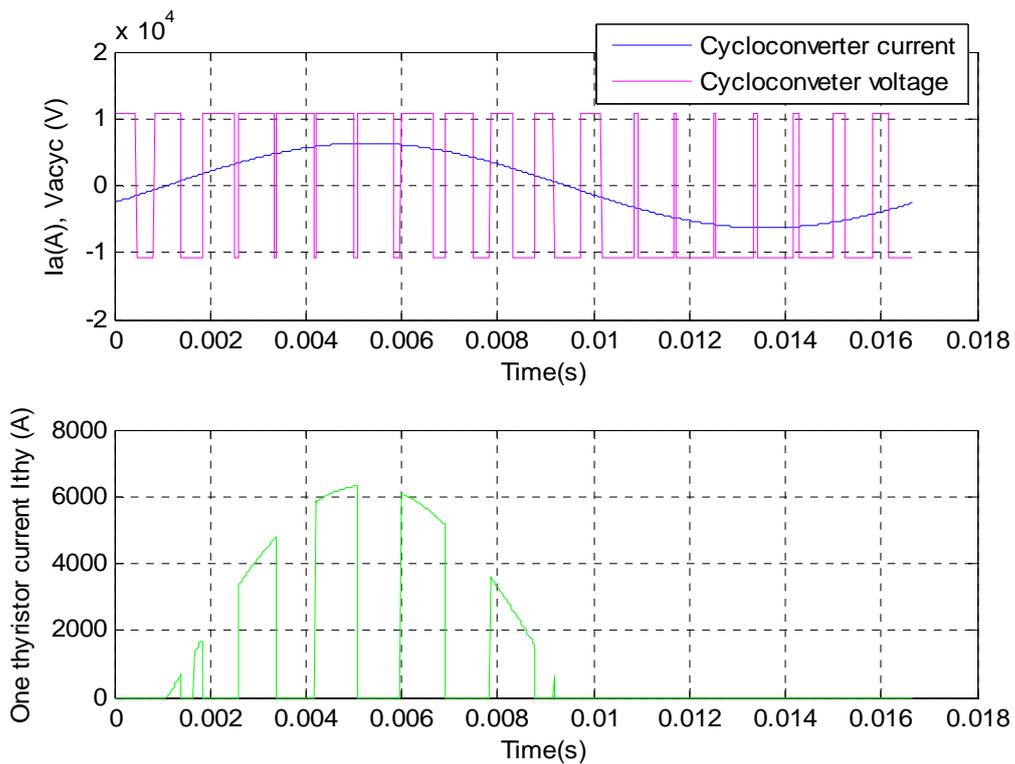

Figure.5.2. simulated waveforms of cycloconverter phase voltage (magenta), current (blue) and one thyristor current (green)
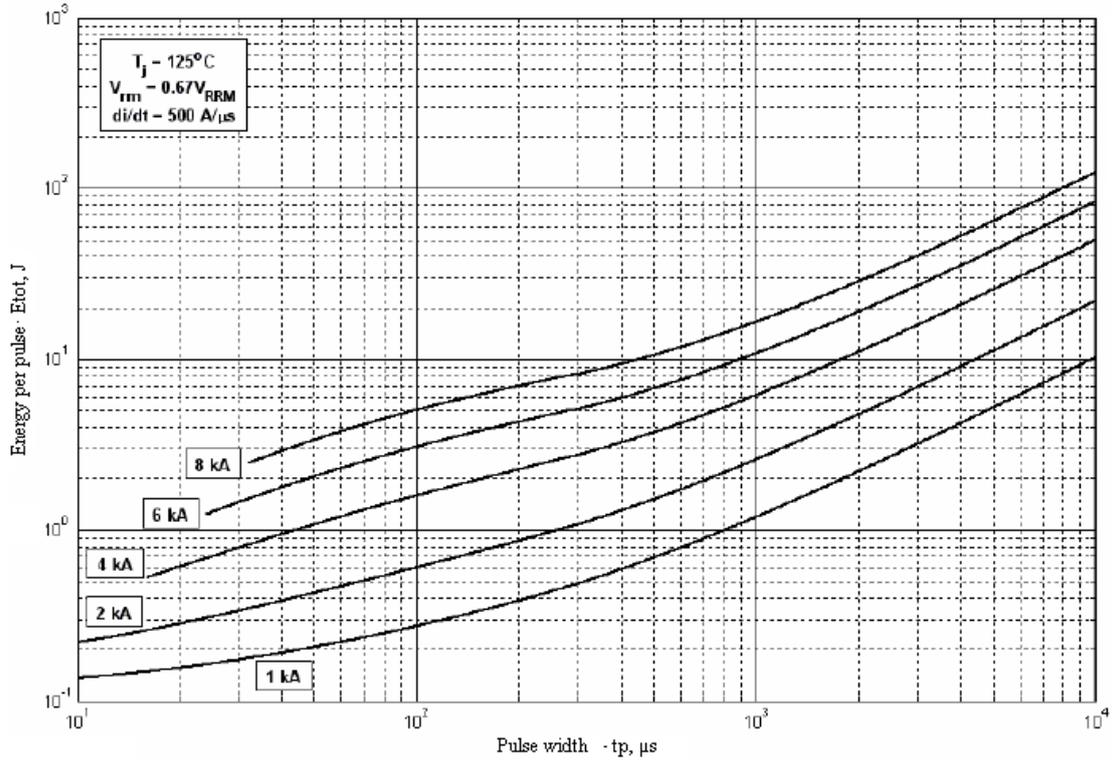
Figure 5.3. Typical total thyristor losses as supplied by thyristor manufacture [14]

The switching losses can be estimated from the difference between the total thyristor losses and the conduction losses using the energy curve above. Thus

the total conduction losses of the cycloconverter are

$$P_{cond,cyc} = 12 N_{thy} P_{cond\_thy}$$ (5.9)

and the total switching losses of the cycloconverter are

$$P_{sw,cyc} = 12 N_{thy} \left(f \sum E_{tot} - P_{cond\_thy} \right)$$ (5.10)

The number of series connected thyristors in the above equations (N_{thy}) can estimated using (4.18).

5.2 Formulation of semiconductor losses for the two-level conventional VSC

The conduction losses per IGBT or diode can be calculated using the same equations as in section 5.1.1. The IGBT turn-off losses can also be calculated using (5.3) and the turn-off energy data from device data sheet. The diode turn-on losses can be ignored since it turns on very quickly, however the IGBT turns on hard in this case and thus the turn-on losses can be calculated by

28

$$P_{igbt\_on} = f \sum E_{on\_igbt}(I_{on\_igbt}) \tag{5.13}$$

The number of IGBTs per valves can be calculated using (4.16), but the total number of the converter IGBTs is different since this converter has six valves (refer to fig 3.11). Thus the total conduction losses of the converter can written as

$$P_{loss\_cond\_vsc} = 6N_{igbt}P_{cond\_igbt} + 6N_{diode}P_{cond\_di} \tag{5.14}$$

Similarly the total switching losses are

$$P_{loss\_sw\_vsc\_hard} = 6N_{igbt}(P_{sw\_igbt} + P_{igbt\_on}) + 6N_{diode}P_{di\_off} \tag{5.15}$$

The subscript ''hard'' stands for hard switching since all the switches turn on and off at when the current through and the voltage across the device are not zero. Therefore, this topology has high switching losses as will be seen later.

5.3 Simulation results, analysis and comparison of semiconductor losses and the volume of the valves

This part presents the simulation results of semiconductors losses and the total volume of the converter valves for the two compared systems. The semiconductor losses and number of devices at different cases where thyristors with different turn-off times used in cycloconverter are shown and compared. Finally, the total volume of the valve installations for both systems are estimated and compared. The simulation has been conducted in Matlab.

The semiconductor losses are expressed in per unit (pu) of the base power of the converter.

5.3.1 Different study cases

Three different cases are studied where thyristors with turn-off times shown in table 5.1 are used in the cycloconverter. These devices are the same as the thyristors shown before in table 4.2. The IGBT data of the VSC part of MCC is given in table 4.4 while the IGBT data of the conventional VSC is given in table 4.6. The switching frequency of the MCC is f_{sw_MCC}=900Hz while the switching frequency of the conventional VSC is taken from [9] as f_{sw_vsc} =1620Hz which is the frequency at which the Valhall offshore converter is designed to operate.

Table5.1 different cases to be studied at $f_{sw\ MCC}$=900Hz and $f_{sw\ vsc}$=1620Hz

Case number	Thyristor module	t_q(μs)	$V_{thy,ssoa}$ (V)	I_{peak}(kA)	$r_T(mΩ)$	$V_T(V)$
1	TF3390-F3-12	10	407	10.65	0.08	1.4
2	TF2910-F2-28	25	936	9.14	0.20	1.4
3	TF 3280-F2-25	40	856	10.30	0.15	1.3

Case1

The semiconductor losses and the number of valves are shown in figure 5.4 and 5.5 respectively. The losses of both VSC and cycloconverter parts of MCC together with the total MCC losses are shown. Comparing the losses of both topologies, it is quite obvious from figure 5.4 that the MCC topology has an inferior loss performance with 0.0216pu compared to 0.0212pu for the VSC topology which means that the losses are increased by about 2.3%

Looking at the distribution of the losses in the MCC topology, it can be seen that the major part of the losses comes from the cycloconverter part as a result of using a large de-rating margin between the maximum blocking voltage (V_{RRM}) and the rated switching safe operating area voltage ($V_{thy,ssoa}$). Therefore, a large number of thyristors is needed to block the voltage applied to cycloconverter valves and the current through these devices is quite high with a peak value of 6335A which is more or less six times the peak current that is handled by the valves of the conventional VSC (1074A). The conduction losses of the cycloconverter are quite high as a result of using thyristors with a low voltage blocking capability. These thyristors have very low switching losses as can be seen in the figure. The diode conduction losses are also quite low in case of using a MCC since its VSC works as inverter and therefore the diodes conduct only for a short time. The IGBTs switching losses are considerably low since they have zero turn-on losses (they turn on at zero current and zero voltage condition) and low turn-off losses as they turn off at zero voltage. The final distribution of the losses is **0.0071pu** for the VSC part of the MCC and **0.0145pu** for the cycloconverter.

On the other hand, it can be seen that the IGBTs have quite high switching losses in case of the conventional VSC topology because this converter employs a hard switching for all semiconductors. The diode losses are lower than those of the IGBT since it conducts for a shorter time.
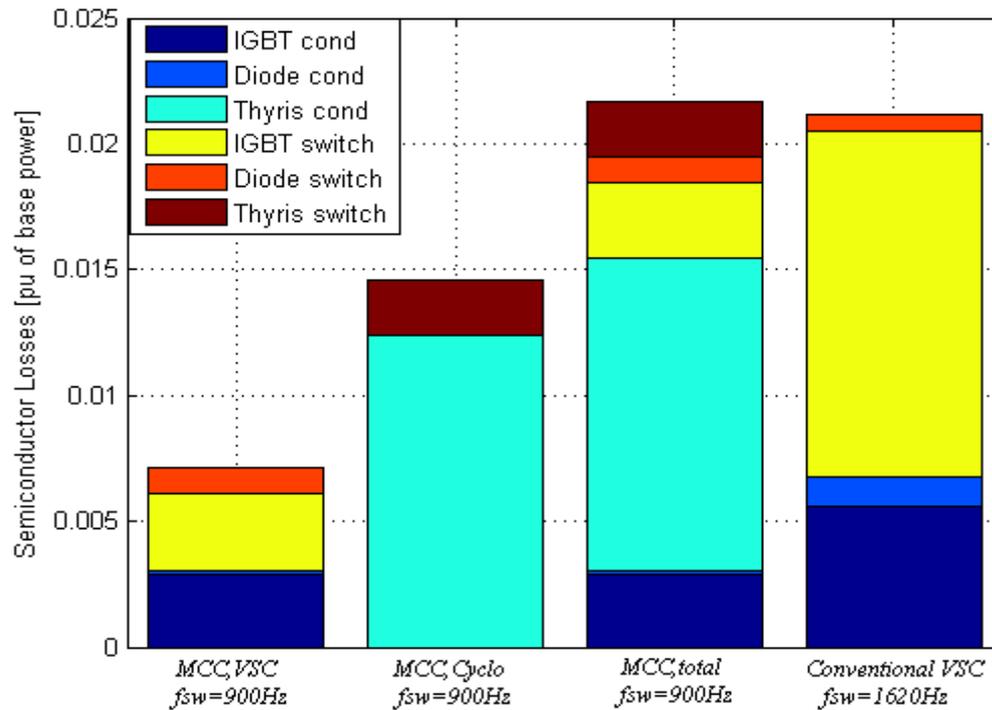
Figure 5.4. Comparison between MCC Losses and conventional VSC losses (right) using fast thyristor TF3390-F3-12 with a t_q=10 µs and V_{RRM}=1200V in MCC cycloconverter

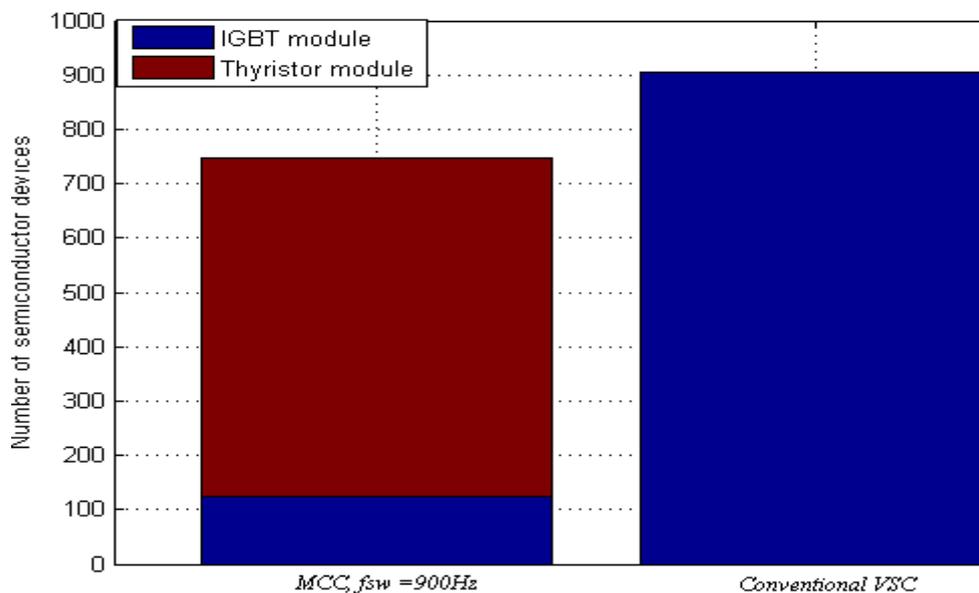*Figure 5.5. Comparison between the number of the switches of the MCC and the conventional VSC (right) using TF3390-F3-12 with a t_q=10 µs and V_{RRM}=1200V in MCC cycloconverter*

It is also of interest to compare the total number of semiconductor devices needed to construct the converter in both cases. It can be seen from figure 5.5 that number of devices in case of the MCC is around 748 (624 thyristors and 124 IGBTs). This number is considerably low compared to the number of devices needed for the conventional VSC which is around 906.

Considering the low cost of thyristors, the MCC topology could result in considerable savings in the investment cost of the converter. However the cost of snubber capacitors for the MCC as well as the cost of the control for both topologies should be taken into consideration when the comparison is made.

Case2

Figure 5.6 and 5.7 show the semiconductor losses and the number of devices respectively. It can be observed that the conduction losses of the cycloconverter are lower than the previous case because the thyristors used in this case have a higher blocking voltage and hence the number of the thyristors is considerably lower as can be seen from the lower figure. Nevertheless, the total MCC losses are slightly higher in this case (0.0223pu) because this type of thyristors have higher switching losses (see fig 5.6) and due to the increase in the losses of the VSC part. The total losses are distributed as 0.0077pu for the VSC part of the MCC and 0.0146pu for the cycloconverter. The increase in the losses of the VSC part of MCC is attributed to the longer turn-off time which implies that a higher transformer turn ratio is needed and hence the transformer current will also be high in this case (refer to section 4.1.3.1). The increase in the total losses of the MCC compared to the conventional VSC topology is roughly around 5.41%.
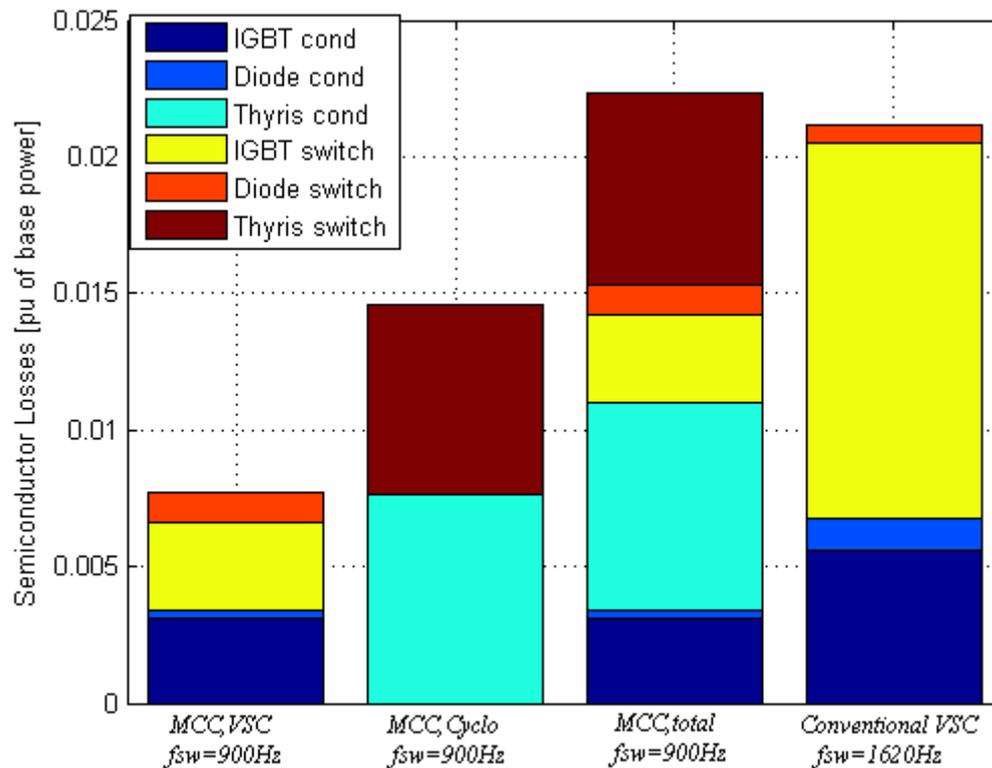

Figure 5.6. Comparison between MCC Losses and conventional VSC losses (right) using fast thyristor TF2910-F2-28 with a t_q=25 µs and V_{RRM}=2800V in MCC cycloconverter
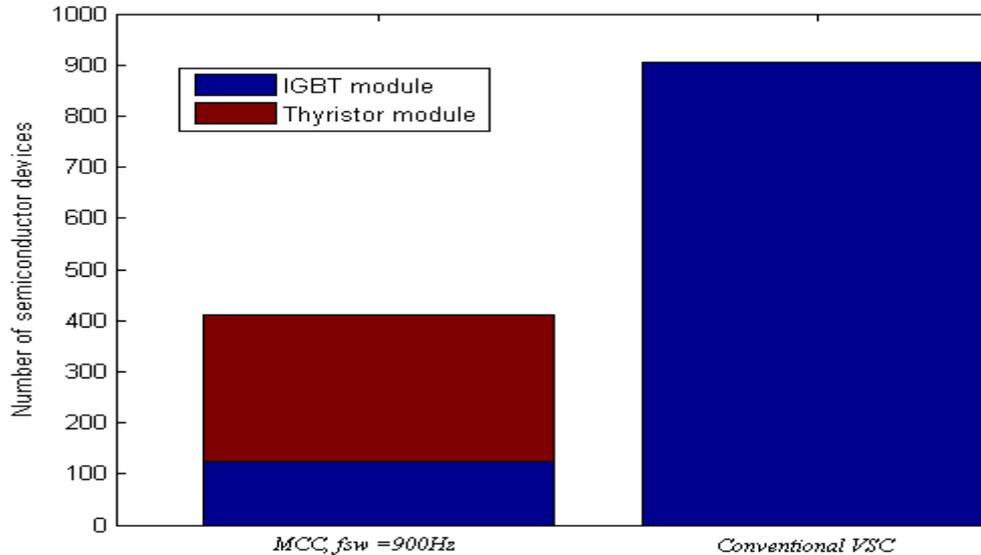
Figure 5.7. Comparison between the number of the switches of the MCC and the conventional VSC using fast thyristor TF2910-F2-28 with a $t_q=25\,\mu s$ and $V_{RRM}=2800V$ in MCC cycloconverter

The total number of MCC devices (288 thyristors+124 IGBT modules) is considerably lower than the previous case which may conclude that this option results in lower investment cost for the MCC compared to the previous one, but with a slight increase in semiconductor losses.

The small number of devices needed to construct the converter together with the small size of MF tranformer could result in a smaller size of the converter station for the MF transformer system in comparison with the LF transformer HVDC system, but this can be confirmed only if there is a clear picture about the valve arrangements, dimensioning and layout of other equipment in both stations.

Case3

In this case a thyristor with a longer turn-off time than those of the two previous cases is applied in the cycloconverter. This thyristor has a blocking voltage higher than the one in case 1 but slightly lower than the one in case 2. Figure 5.8 and 5.9 show a comparison between the losses and the number of semiconductor devices for the two systems respectively.

In this case the semiconductor losses of the VSC part of MCC (0.0084pu) are higher than the two previous cases for the same reason discussed in paragraph 5.1.3.2.
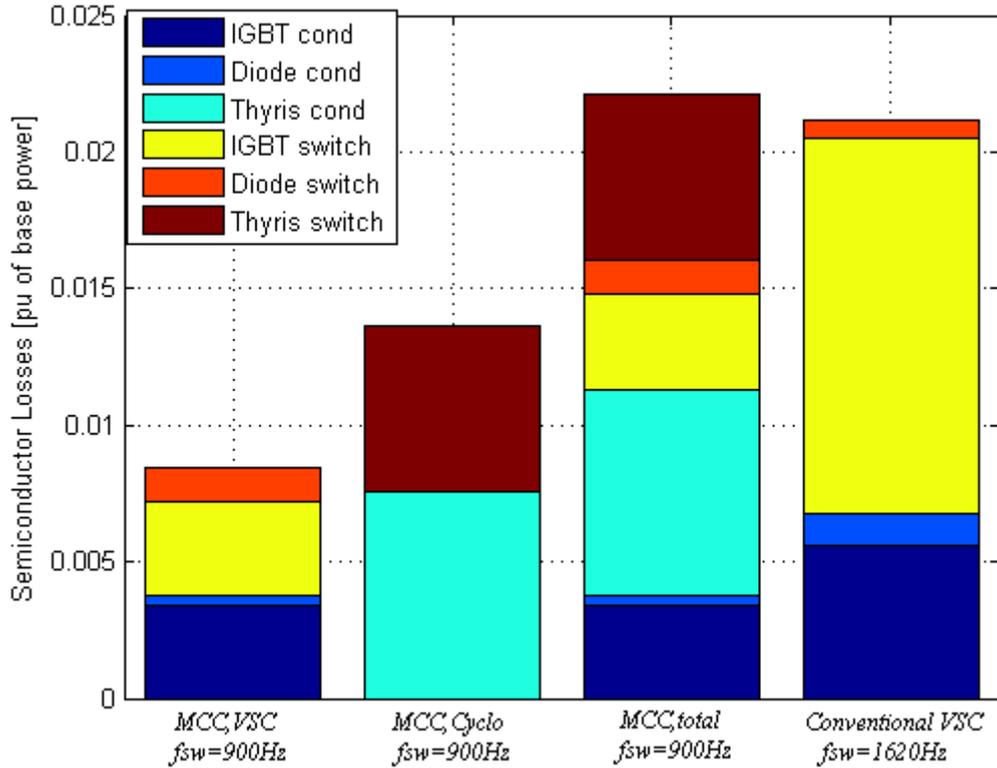
Figure 5.8. Comparison between MCC Losses and conventional VSC losses (right) using fast thyristor TF3280-F2-25 with a t_q=40 µs and V_{RRM}=2000V in MCC cycloconverter
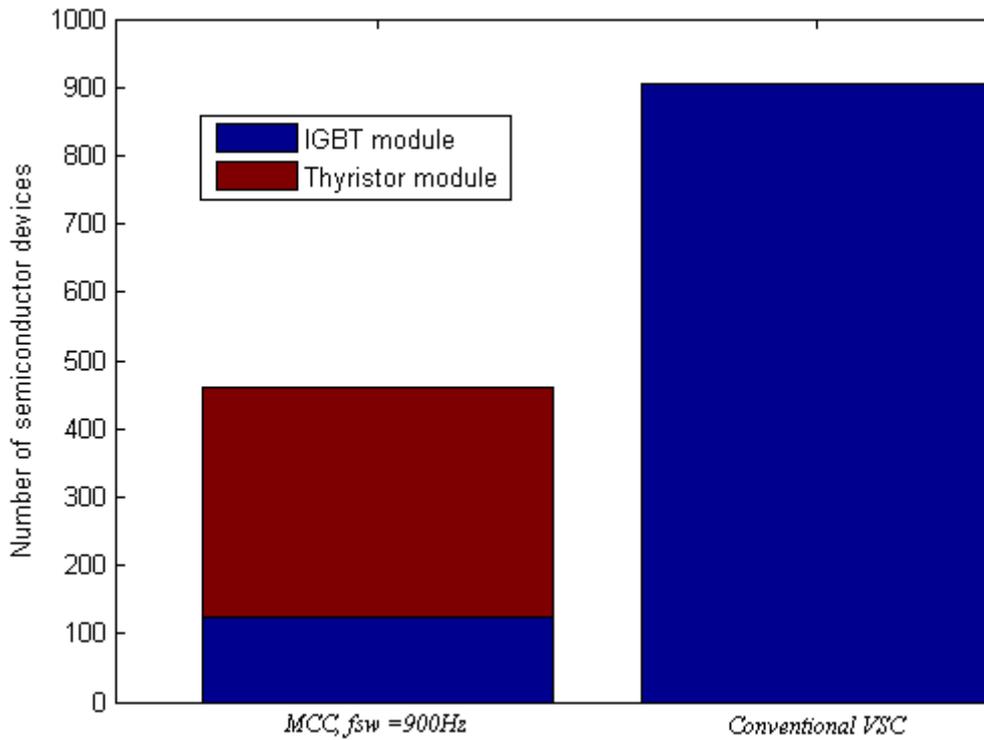

Figure 5.9. Comparison between the number of the switches of the MCC and the conventional VSC using fast thyristor TF3280-F2-25 with a t_q=40 µs and V_{RRM}=2000V in MCC cycloconverter

The total losses of MCC are 0.0221pu which consist of 0.0084pu for the VSC part and 0.0137pu for the cycloconverter. The cycloconverter losses are lower than the previous case because of using a thyristor with a lower threshold voltage and lower switching losses. The percentage of the increase in the MCC losses is around 4.47%.The total number of MCC devices is 460 (336 thyristors+124 IGBT modules) compared to 906 for the conventional VSC.

Summary of the results for the three studied cases

Table 5.2 and figure 5.10 give a summary of the calculated results for the above discussed cases

Table 5.2 summary of the results for the three cases

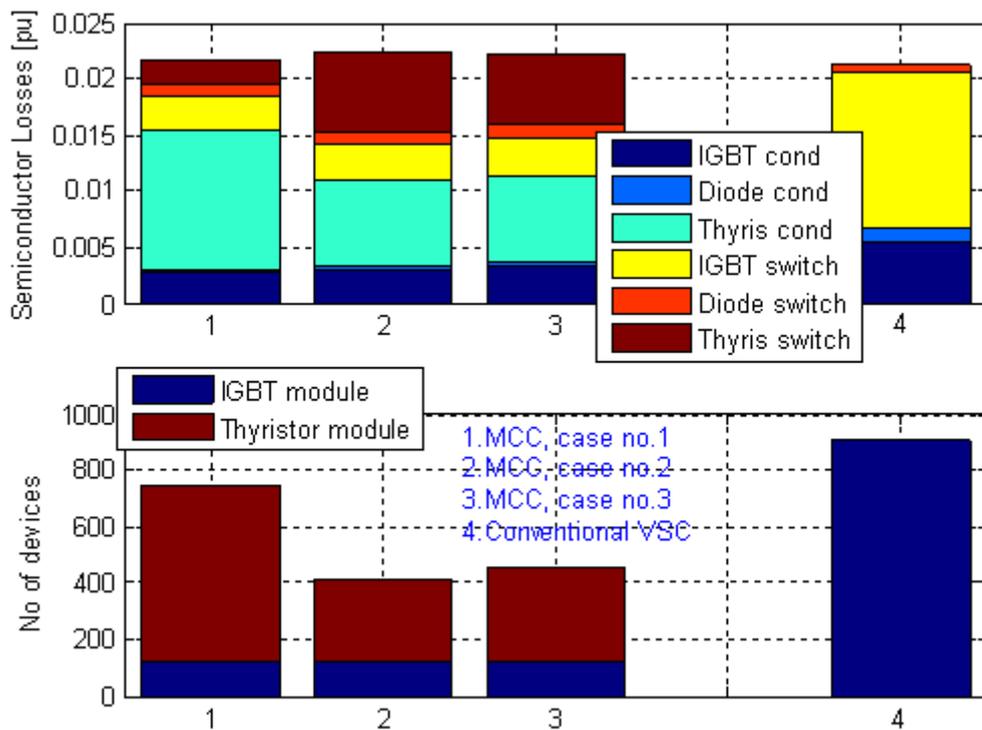| Case No	MCC Losses [pu] f_{sw}=900Hz		Conventional VSC losses[pu], f_{sw}=1620Hz	% of loss increase	Number of MCC devices	Number of devices for conventional VSC
	VSC	Cycloconverter				
1	0.0071	0.0145	0.0212	2.30	748	906
2	0.0077	0.0146	0.0212	5.41	412	906
3	0.0084	0.0137	0.0212	4.47	460	906

Figure 5.10. Semiconductor losses and number of devices for the three discussed cases

Comparing the three options discussed above (refer to fig 5.10), it can be noticed that the switching losses increase with the increase of the blocking voltage of the thyristor. This can also be observed by comparing the energy curves of these thyristors found in appendix A.

From the table and the plot, it is obvious that the thyristor with the lowest blocking voltage and shortest turn-off time (case 1) has the best loss performance, but the number of thyristors required to construct the converter are considerably higher compared to the other two cases.

Considering the number of devices needed to construct the cycloconverter and the slight loss difference between three cases, it would be fair to recommend the choice of thyristors with the highest blocking voltage (like the one in case2) if the converter is intended to be used in offshore environment as this option could result in a smaller size of the converter which is a crucial factor in offshore applications

5.3.3 The total volume of the valve installations

The volume of the of the conventional VSC valves

Figure 5.11 shows a rough sketch of the conventional VSC valves as they arranged in the Valhall offshore station [19]. The three converter legs are tagged by the letters A, B and C. For simplicity, the cooling water pipes which run along the upper part of the valve ceiling are ignored in this drawing and they will not be considered in the calculation of the total space occupied by the valves. There are two valves in each leg and each valve consists of 151 series-connected IGBT modules arranged in a number of layers. The valve structure is suspended from the ceiling of the valve hall via porcelain insulators. The valve clearance (distance from the ground) is around 1.26m and the total space occupied by the valve installation is found to be roughly around 461m^3.
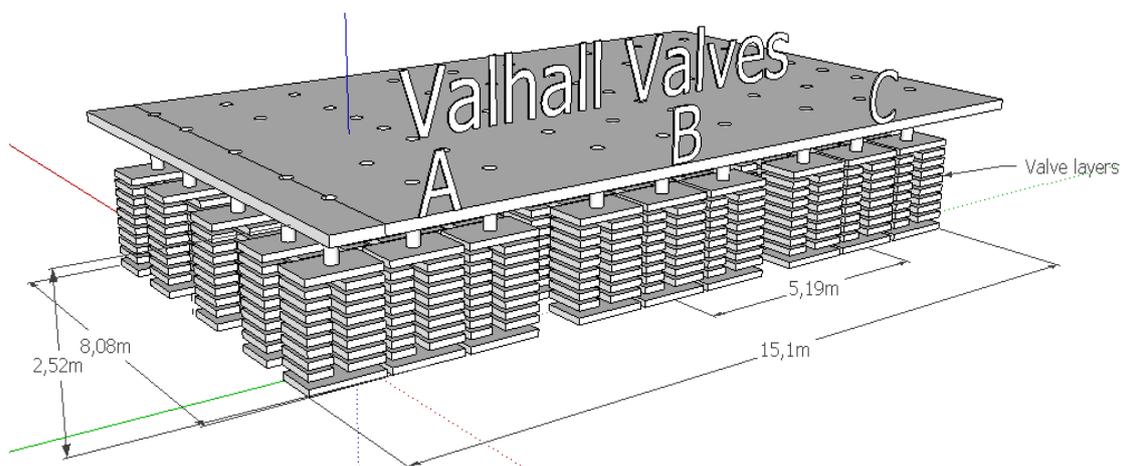

Figure 5.11.The arrangements of the conventional VSC valves

The volume of the MCC valves

The valve arrangements of the VSC part of the MCC are diagramed in figure 5.12. Each valve consists of 62 series-connected IGBT modules and snubber capacitors. Since the converter has only one leg, the total number of the VSC devices is around

124. The valve clearance is around 1.26m. A rough estimation of the total space occupied by the installation results in a value of **138m³**
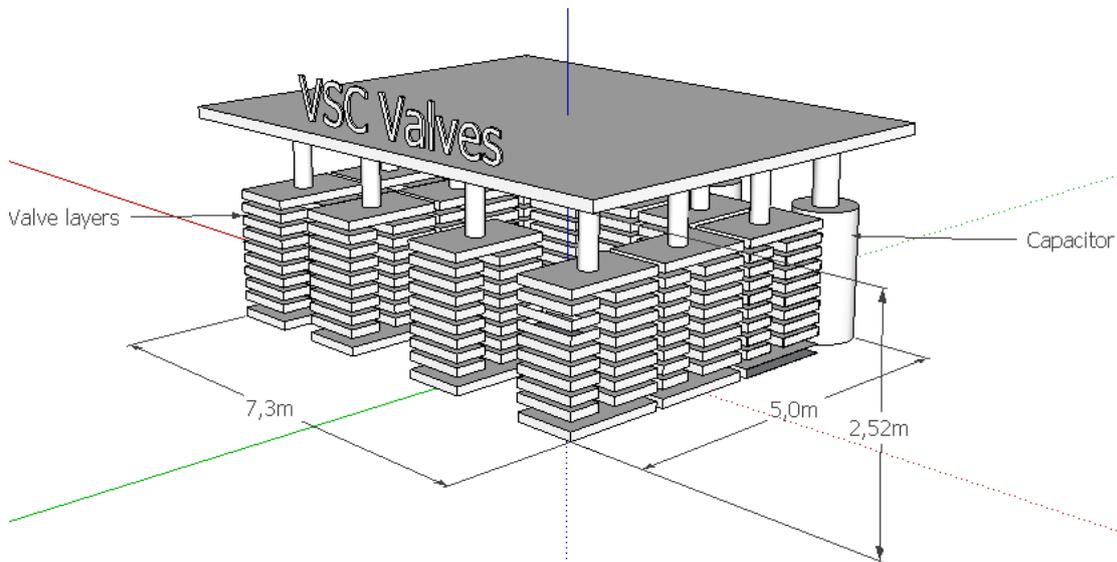

Figure 5.12.The arrangements of the MCC VSC valves

Figure 5.13 shows a rough sketch of the cyclocnverter valves. For simplicity, the thyristor layers in each valve are shown as a black box which has a similar volume as the layers in the corresponding valve and the water pipes running across the upper part of the valves are ignored. The number of the series-connected thyristors per valve is around 24 thyristors and the total number of the thyristors in the cycloconverter is around 288 thyristors. This valve design is based on the thyristor TF2910-F2-28 (case no.2) presented in paragraph 5.3.1. The total occupied space in this case is roughly around **19.5m³**.
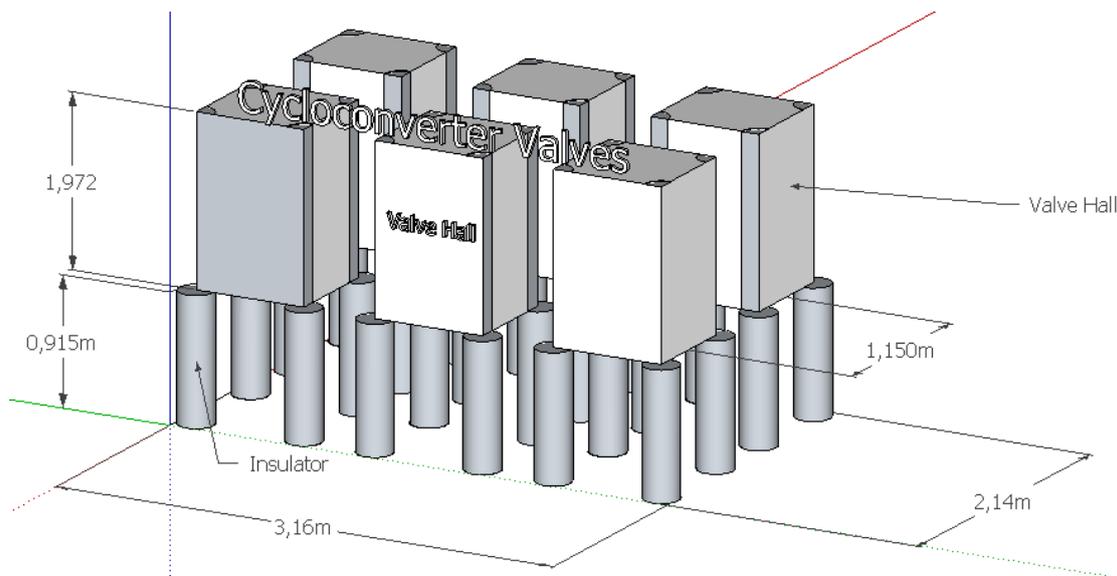

Figure 5.13.Schematic diagram of the MCC cycloconverter valves

The above dimensions have been made according to the dimensioning drawing of the SVC classic [20]. The total space occupied by the MCC valves is around 157.5m³.

This value is approximately around **34 %** of the space occupied by the conventional VSC valves.

Chapter 6
Conclusions and Future Work

This chapter summarizes the work in this thesis and puts forward future aims in this field.

6.1 Conclusions

In this thesis the semiconductor ratings of two different HVDC systems are determined and their losses and the size of the valves are compared. It is found that the MF transformer system requires a less number of semiconductor devices. The size of the installation of the MCC valves is found approximately around **34%** of the size of the conventional VSC valves. However, the semiconductor losses in this case will be higher by around **5%** which may conclude that the use of the MF transformer HVDC system could be more feasible in an application where the size of the converter station is of concern.

Using a one-leg MCC VSC, implemented with high blocking voltage devices, results in a significant reduction in the number of IGBTs. The number of devices in the cycloconverter is also reduced despite the low rated SSOA voltage of the thyristors since the cycloconverter valves are required to block a much lower voltage than the one blocked by the VSC valves as the primary voltage of the MF transformers is scaled down first before it is applied to the cycloconverter. These two factors combined together result in a less number of semiconductor devices for the MF HVDC system and, as a result, a small size of the valves.

Fast thyristors with different turn-off times and blocking voltages have been investigated in this study. A trade-off between the number of thyristors needed to construct the cycloconverter part of the MF transformer system and the devices losses should be made. The simulation results have shown that it is better to implement the cycloconverter using thyristors with a higher blocking voltage and a relatively short turn-off time (case2) as long as the size of the converter is of concern. This option could lead to a smaller volume of the valves and, as a result, the size of the converter station could be substantially reduced which is strongly needed in offshore environment and city centre in-feed.

6.2 Future Work

The MCC semiconductor losses have been calculated without considering the ripple in the AC side current which implies that the loss figures are not evaluated accurately. Therefore, a detailed dimensioning of the AC side of the MF HVDC system is required especially the design of the reactor and shunt filter using the exact grid impedance at different frequencies and taking the required harmonics limits into account. The real AC side current can be calculated based on this design and hence it is possible to get the exact simulated loss figures. These loss figures should be verified by measurements since the thyristor manufactures do not supply separate energy curves for the device switching losses. This implies that the simulated thyristor switching losses are just an estimated value.

The size and weight of the station components is an important figure for both systems for offshore application. Therefore, a detailed dimensioning of the LF transformer, MF transformer, shunt filters and phase reactors is required to determine the overall volume of equipment and to have a clear picture of the converter station layout for both systems.

Bibliography

[1] Staffan Norrga, "On Soft-Switching Isolated AC/DC Converters without Auxiliary Circuit", Doctoral Thesis in Royal Institute of Technology, April 2005.

[2] Staffan Norrga, "Modulation Strategies for Mutually Commutated Isolated Three-Phase Converter Systems." 36th IEEE Power Electronics Specialists Conference, June 2005.

 [3] Stephan Meier, Staffan Norrga, Hans-Peter Nee "Modulation Strategies for a Mutually Commutated Converter System in Wind Farms", Proceedings EPE 2007, September 2007.

[4] Stephan Meier, Staffan Norrga, Hans-Peter Nee, "Control Strategies for Mutually Commutated Converter Systems without Cycloconverter turn-off Capabilities'', Proceedings IEEE Power Electronics Specialists Conference, June 2008.

[5] Stephan Meier, "Novel Voltage Source Converter based HVDC Transmission System for offshore Wind Farms'', Licentiate thesis, KTH, 2005.

[6] S.Meier, S.Norrga, H.-P.Nee "New Voltage Source Converter Topology for HVDC Grid Connection of Offshore Wind farms'', Proceedings of EPE-PEMC 04, September 2004.

[7] Stephan Meier, "System Aspects and Modulation Strategies of a New HVDC Transmission System for Wind Farms'', PhD Thesis, KTH, May 2009.

[8] Jonas Lindgren, "Valhall Re-development project, Main Circuit Parameters'', document no: PH-AS-E-0009, Technical Report, ABB, April 2006.

[9]. Jonas Lindgren, "Valhall Re-development project, AC Filter Design, Document'', no: PH-AS-E-0013, Technical Report, ABB, April 2006.

[10] Jonas Lindgren, "Valhall Design Basis Report'', Document no**:** 1JNL100099-010, Technical Report, ABB, June 2004.

[11] Jon Rasmussen, Hans-Olla-Bjarme, "Valhall Re-development project, Electrical design report for Valhall'', document no: 1JNL100101-264, Rev 05, ABB, August 2004

 [12] Zhao Shuang, "Mutually commutated converter equipped with thyristor-based cycloconverter", M. Sc. Thesis, Chalmers, 2008.

[13]Ned Mohan, Tore M.Undeland, William P.Robbins, "Power Electronics Converters, Applications and Design'', Third Edition, John Wiley& Sons, 2003

[14] www.eur.proton-electrotex.com

[15]Project Light C, "5.2kV 2000A soft switching IGBT main device specifications'', ABB Switzerland

[16] "IGBT-Presspack 5SNA 130025H0003 PG4 Light B specifications'', ABB Switzeland

[17] http://www.westcode.com/dgt.htm

[18] Baoliang Sheng, Hans-Ola Bjarme, "Type Test Assesment of Jeddah SVC Project PCT TCR Valves'', Document no: 1JNL 100110-989, 2006

[19] Olle Ekwal, Håkan Andersson, Patrik Karlson, "Dimensioning drawing of Valhall valves'', September 2007

[20] Ida Hägerlund, Hans Johansson, K-O Eriksson, "Dimensioning Drawing, TCR valve PCT 6-22 levels long insulators'', SVC Classic Project, February 2009

Appendices

Appendix A

Thyristors Energy curves

In this part the energy curves that describe total thyristor losses as supplied by manufacture are shown.
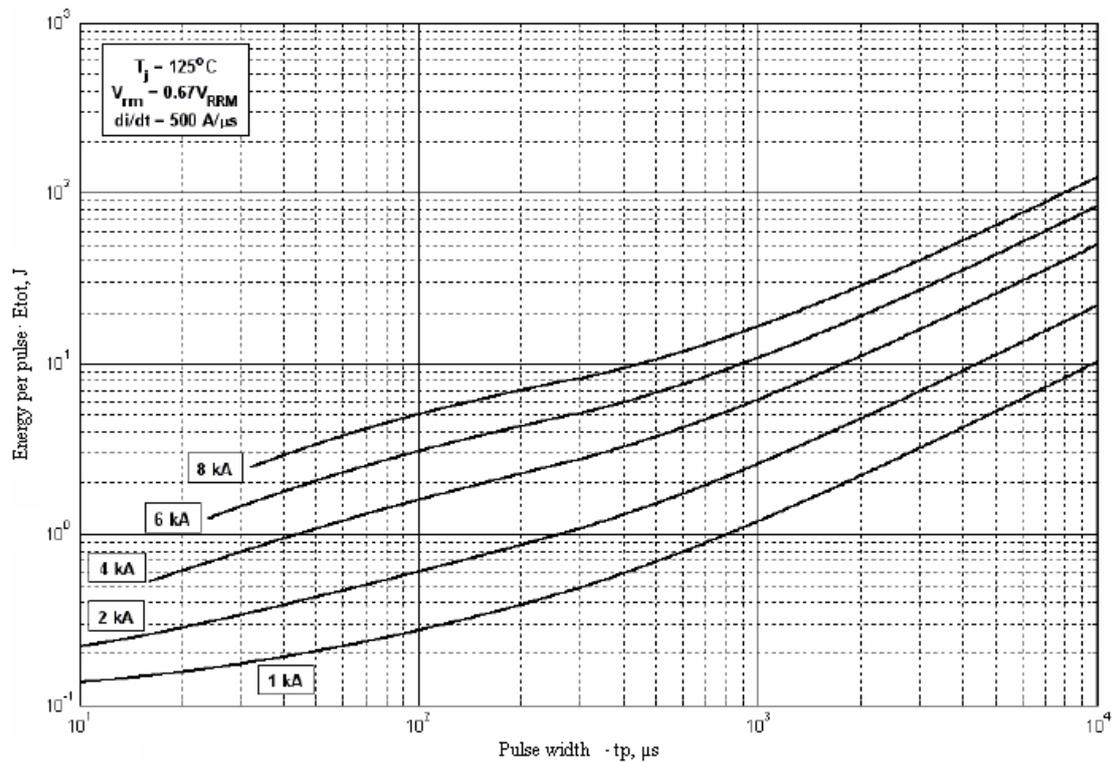
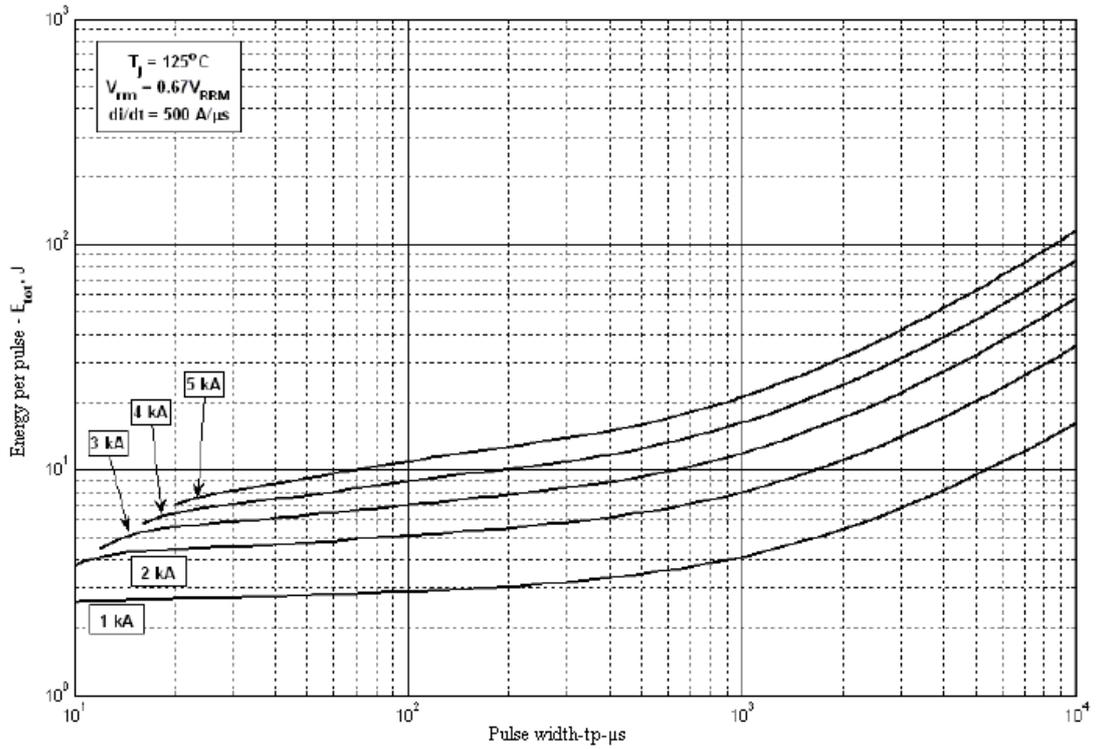*Figure A1. Total energy per pulse for the fast thyristor TF3390-F3-12 which has a V_{RRM}=1500V and tq=10μs [14]*

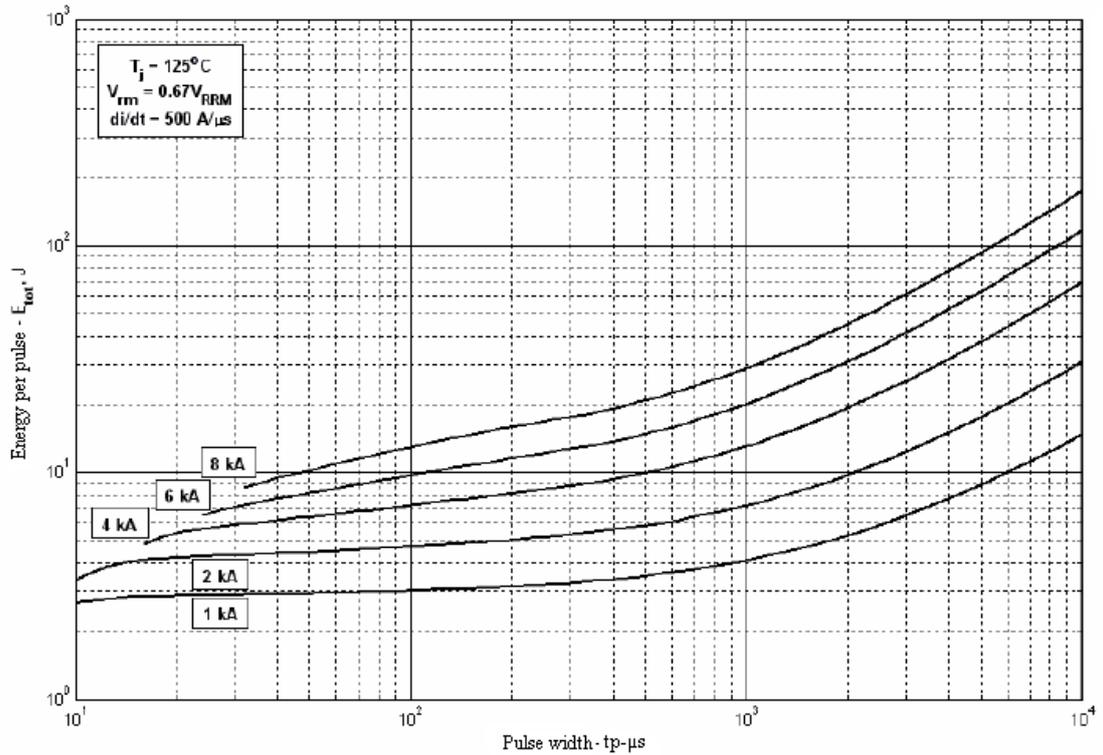*Figure A2. Total energy per pulse for the fast thyristor TF2910-F2-28 which has a V_{RRM}=2800V and t_q=25μs [14]*

Figure A3. Total Energy per pulse for the fast thyristor TF3280-F2-25 which has a V_{RRM}=2500V and tq=40μs [14]

44

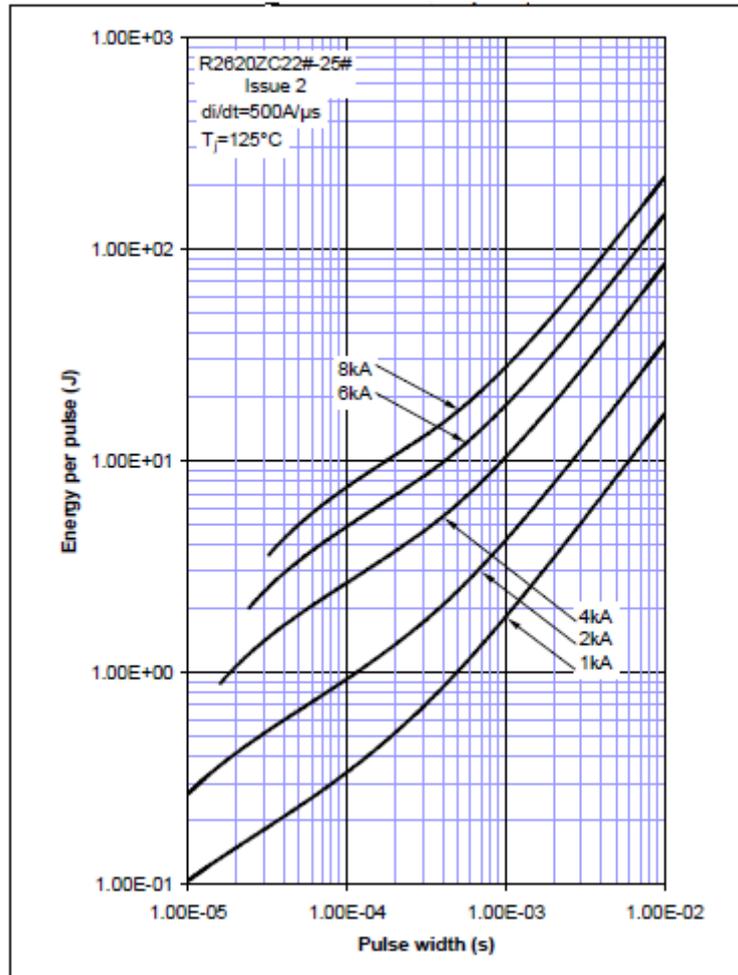*Figure A4. Total energy per pulse for the fast thyristor R2620ZC22 which has a V$_{RRM}$=2500V and tq=50µs [17]*

Appendix B

Loss comparison using thyristors from different manufactures
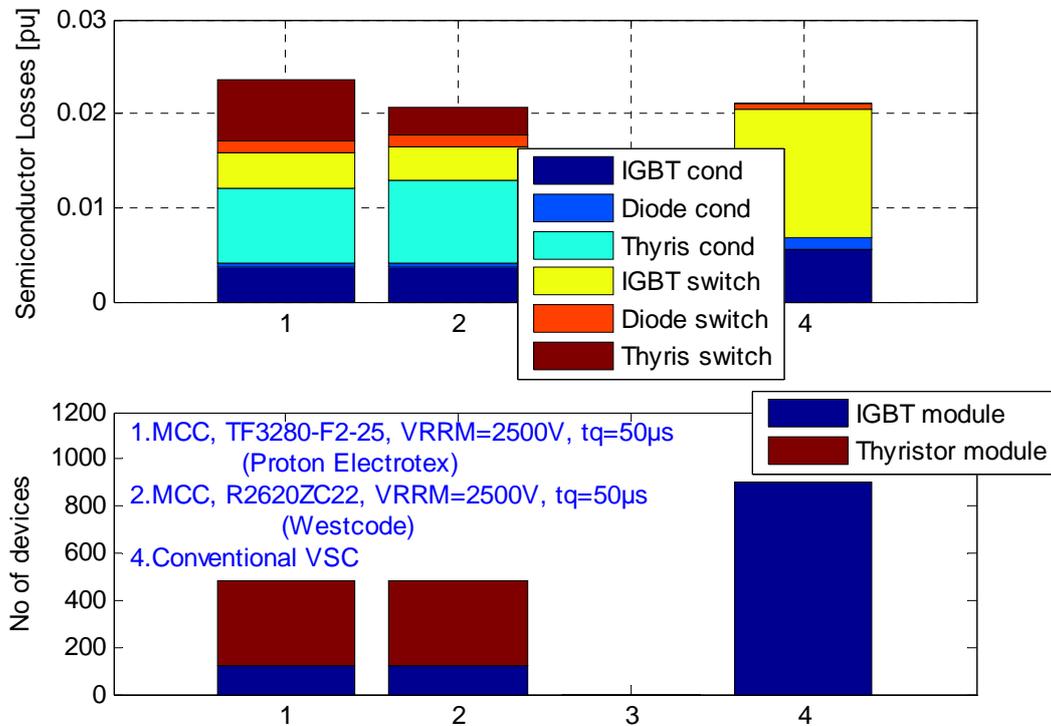

Figure B.1. Comparison between the semiconductor losses and the number of the devices for the MCC and the conventional using thyristors from different manufactures. The switching frequencies are f_{sw_MCC} =900Hz and f_{sw_vsc}=1620Hz for the MCC and the conventional VSC respectively. The total number o f MCC devices=484, the loss increase=11% using Proton-Electrotex thyristor and -2.2% using Westcode thyristor.

Table B.1. Characteristics of fast thyristors TF3280-F2-25 (Proton Electrotex [14]) and R2620ZC22 (Westcode [17]) used in the plot of fig.B.1 and B2

Thyristor module	TF3280-F2-25	R2620ZC22
Mean on-state current (half sine wave)	3280A	2620A
Repetitive peak off-state voltage V_{DRM}	2500V	2500V
Repetitive peak reverse voltage V_{RRM}	2500V	2500V
Rated SSOA voltage $V_{thy,ssoa}$	836V	836V
Turn-off time t_q	50 μs	50μs
On-state threshold voltage V_T	1.3V	1.5V
On-state slop resistance r_T	0.15 mΩ	0.163mΩ

MCC losses and number of devices at different switching frequencies using different fast thyristors
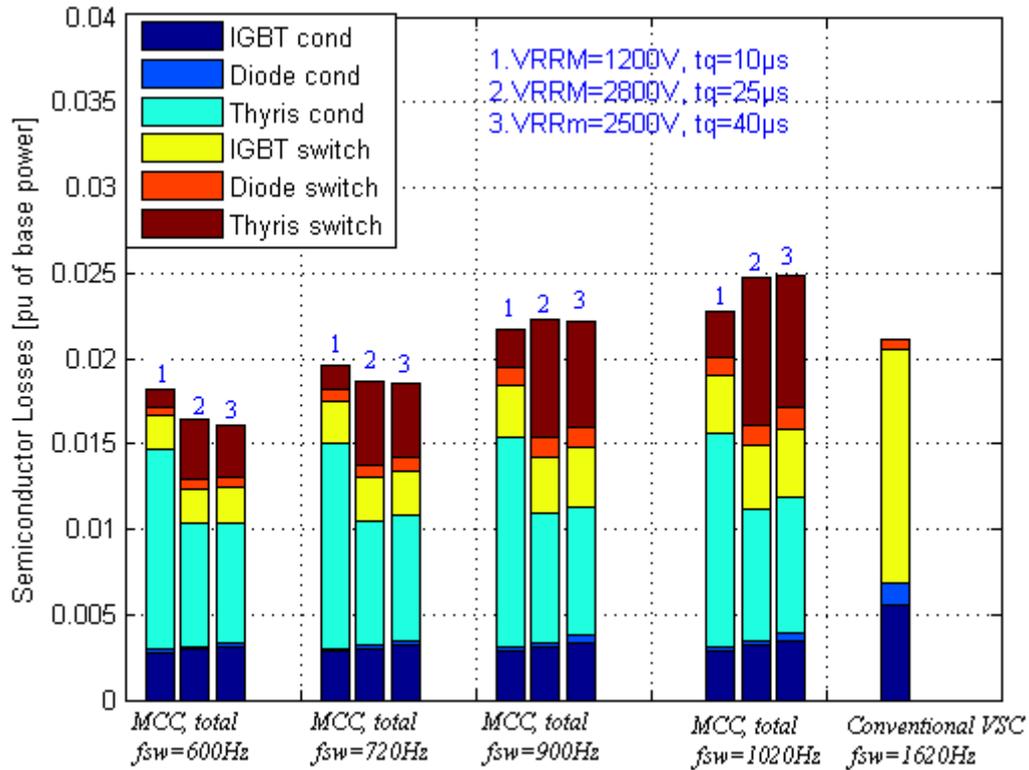

Figure B.2. Comparison between MCC losses and conventional VSC losses using different fast thyristors in MCC cycloconverter at different switching frequencies for the MCC.
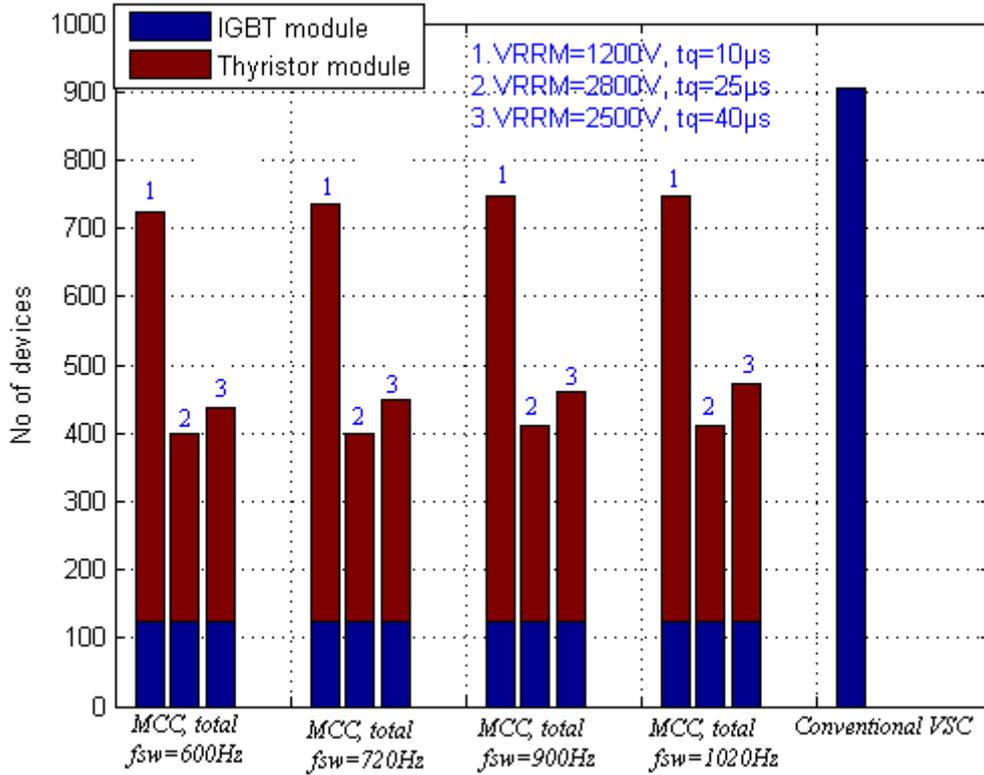
Figure B.3. Comparison between the number of MCC devices and conventional VSC devices using different fast thyristors in MCC cycloconverter at different switching frequencies for the MCC.